



**Calhoun: The NPS Institutional Archive**  
**DSpace Repository**

---

Theses and Dissertations

1. Thesis and Dissertation Collection, all items

---

1994-03

Mach number, flow angle, and loss  
measurements downstream of a transonic  
fan-blade cascade

Austin, Jeffrey G.

Monterey, California. Naval Postgraduate School

---

<http://hdl.handle.net/10945/30868>

---

This publication is a work of the U.S. Government as defined in Title 17, United States Code, Section 101. Copyright protection is not available for this work in the United States.

*Downloaded from NPS Archive: Calhoun*



Calhoun is the Naval Postgraduate School's public access digital repository for research materials and institutional publications created by the NPS community. Calhoun is named for Professor of Mathematics Guy K. Calhoun, NPS's first appointed -- and published -- scholarly author.

**Dudley Knox Library / Naval Postgraduate School**  
**411 Dyer Road / 1 University Circle**  
**Monterey, California USA 93943**

<http://www.nps.edu/library>

NAVAL POSTGRADUATE SCHOOL  
Monterey, California



# THESIS

MACH NUMBER, FLOW ANGLE, AND LOSS MEASUREMENTS  
DOWNSTREAM OF A TRANSONIC FAN-BLADE CASCADE

By  
Jeffrey G. Austin  
March 1994

Thesis Advisor:

Raymond P. Shreeve

Approved for public release; distribution is unlimited

Thesis  
A97145

NAVAL POSTGRADUATE SCHOOL  
MONTEREY CA 93943-5101

## REPORT DOCUMENTATION PAGE

Form Approved  
OMB No. 0704-0188

1a. REPORT SECURITY CLASSIFICATION Unclassified		1b. RESTRICTIVE MARKINGS	
2a. SECURITY CLASSIFICATION AUTHORITY		3. DISTRIBUTION/AVAILABILITY OF REPORT Approved for public release; distribution is unlimited	
2b. DECLASSIFICATION/DOWNGRADING SCHEDULE		4. PERFORMING ORGANIZATION REPORT NUMBER(S)	
6a. NAME OF PERFORMING ORGANIZATION Naval Postgraduate School		6b. OFFICE SYMBOL (If applicable)	
6c. ADDRESS (City, State, and ZIP Code) Monterey, CA 93943-5000		7a. NAME OF MONITORING ORGANIZATION Naval Postgraduate School	
8a. NAME OF FUNDING/SPONSORING ORGANIZATION Naval Air Warfare Center Aircraft Division		8b. OFFICE SYMBOL (If applicable)	
8c. ADDRESS (City, State, and ZIP Code) P.O. Box 7176 Trenton, NJ 08628-0176		7b. ADDRESS (City, State, and ZIP Code) Monterey, CA 93943-5000	
9. PROCUREMENT INSTRUMENT IDENTIFICATION NUMBER N6237693WR00051		10. SOURCE OF FUNDING NUMBERS	
		PROGRAM ELEMENT NO. WR024	PROJECT NO. 03
		TASK NO. 001	WORK UNIT ACCESSION NO.
11. TITLE (Include Security Classification) MACH NUMBER, FLOW ANGLE, AND LOSS MEASUREMENTS DOWNSTREAM OF A TRANSONIC FAN-BLADE CASCADE.(UNCLASSIFIED)			
12. PERSONAL AUTHOR(S) Austin, Jeffrey G.			
13a. TYPE OF REPORT Master's Thesis	13b. TIME COVERED FROM _____ TO _____	14. DATE OF REPORT (Year, Month, Day) March 1994	15. PAGE COUNT 85
16. SUPPLEMENTARY NOTATION The views expressed in this thesis are those of the author and do not reflect the official policy or position of the Department of Defense or the U.S. Government.			
17. COSATI CODES		18. SUBJECT TERMS (Continue on reverse if necessary and identify by block number)	
FIELD	GROUP	SUB-GROUP	
		Shock-Boundary Layer Interaction, Transonic Fan Simulation, Boundary Layer Separation	
19. ABSTRACT (Continue on reverse if necessary and identify by block number) Two dimensional flow measurements of Mach number and flow angle were conducted downstream of a transonic fan-blade cascade at a Mach number of 1.4 to provide baseline data for assessing the effect of vortex generating devices on the suction surface shock-boundary layer interaction. The experimental program consisted of the design and calibration of a traversing three-port pneumatic probe to measure Mach number and flow angle and initial cascade measurements to provide baseline data for the fully-mixed-out total pressure loss coefficient and flow turning angle. Similar tests are planned with the vortex generating devices installed. Comparisons with and without the vortex generating devices are needed to quantify the overall effect on the shock-boundary interaction in a transonic fan-blade passage, and to assess the potential for using vortex generating devices in military engine fans.			
20. DISTRIBUTION/AVAILABILITY OF ABSTRACT <input checked="" type="checkbox"/> UNCLASSIFIED//UNLIMITED <input type="checkbox"/> SAME AS RPT. <input type="checkbox"/> DTIC USERS		21. ABSTRACT SECURITY CLASSIFICATION Unclassified	
22a. NAME OF RESPONSIBLE INDIVIDUAL Raymond P. Shreeve		22b. TELEPHONE (include Area Code) (408) 656 - 2593	22c. OFFICE SYMBOL AA/SF

Approved for public release; distribution is unlimited.

Mach Number, Flow Angle, and Loss Measurements Downstream of a Transonic  
Fan-Blade Cascade

by

Jeffrey G. Austin  
Lieutenant, United States Navy  
B.S., University of Puget Sound, 1985


Submitted in partial fulfillment of the requirements for  
the degree of

MASTER OF SCIENCE IN AERONAUTICAL ENGINEERING

from the


NAVAL POSTGRADUATE SCHOOL  
March 1994


Author:

  
U Jeffrey G. Austin

Approved by:

  
Raymond P. Shreeve, Thesis Advisor

  
U Garth V. Hobson, Second Reader

  
Daniel J. Collins, Chairman,  
Department of Aeronautics and Astronautics

## ABSTRACT

Two dimensional flow measurements of Mach number and flow angle were conducted downstream of a transonic fan-blade cascade at a Mach number of 1.4 to provide baseline data for assessing the effect of vortex generating devices on the suction surface shock-boundary layer interaction. The experimental program consisted of the design and calibration of a traversing three-port pneumatic probe to measure Mach number and flow angle and initial cascade measurements to provide baseline data for the fully-mixed-out total pressure loss coefficient and flow turning angle. Similar tests are planned with the vortex generating devices installed. Comparisons with and without the vortex generating devices are needed to quantify the overall effect on the shock-boundary interaction in a transonic fan-blade passage, and to assess the potential for using vortex generating devices in military engine fans.

## TABLE OF CONTENTS

I.	INTRODUCTION .....	1
II.	EXPERIMENTAL DEVELOPMENTS.....	4
	A. PROBE DESIGN.....	4
	B. PROBE CALIBRATION.....	5
	1. Data Acquisition System.....	7
	2. Program of Measurements .....	7
	3. Probe Characteristics .....	8
	4. Application of the Calibration.....	11
	C. TRANSONIC CASCADE MODEL AND DATA ACQUISITION .....	12
	1. Transonic Cascade Model .....	12
	2. Data Acquisition System.....	14
III.	EXPERIMENTAL PROGRAM, RESULTS AND DISCUSSION .....	16
	A. EXPERIMENTAL PROGRAM .....	16
	B. REPEATABILITY TESTS.....	17
	C. TURNING ANGLE DISTRIBUTION .....	19
	D. PROBE STATIC PRESSURE DISTRIBUTION.....	20
	E. MODEL BASELINE MEASUREMENTS .....	21

IV. CONCLUSIONS AND RECOMMENDATIONS.....	30
APPENDIX A. PROGRAM "CAL_ACQ" .....	33
APPENDIX B. PROBE CALIBRATION RAW DATA .....	37
APPENDIX C. APPLICATION OF THE CALIBRATION.....	39
APPENDIX D. PROGRAM "NEW_READ_ZOC1" .....	46
APPENDIX E. MIXED-OUT LOSS CALCULATION .....	60
APPENDIX F. SELECTED RAW DATA.....	64
LIST OF REFERENCES .....	70
INITIAL DISTRIBUTION LIST.....	72



## LIST OF TABLES

TABLE 1.	PROBE CALIBRATION COEFFICIENTS.....	11
TABLE 2.	REPEATABILITY TESTS 2/24/94 RUN 2 AND RUN 4....	17
TABLE 3.	MEASURED PRESSURES AND PORTS ASSIGNED.....	22
TABLE 4.	PROBE TRAVERSE POSITION .....	22
TABLE 5.	BASELINE TUNNEL CONDITIONS .....	23
TABLE 6.	BASELINE FULLY-MIXED-OUT CONDITIONS .....	23
TABLE B1.	PROBE CALIBRATION RAW DATA X = 0.10 - 0.22.....	37
TABLE B2.	PROBE CALIBRATION RAW DATA X = 0.26 - 0.37.....	38
TABLE C1.	CALIBRATION METHOD RESULTS X = 0.10 - 0.22.....	44
TABLE C2.	CALIBRATION METHOD RESULTS X = 0.26 - 0.37.....	45

## LIST OF FIGURES

Figure 1.	Shock-Boundary Layer Interaction .....	1
Figure 2.	Low-Profile Vortex Generator .....	2
Figure 3.	Probe Tip Enlarged.....	4
Figure 4.	Free-Jet Calibration Apparatus.....	6
Figure 5.	Probe Holder Assembly .....	6
Figure 6.	Beta Characteristic .....	9
Figure 7.	Gamma Characteristic .....	9
Figure 8.	Wind Tunnel Facility.....	13
Figure 9.	Transonic Cascade Model Test Section.....	13
Figure 10.	Cascade Blading Geometry .....	15
Figure 11.	Blade Wake Survey: 2/24/94 Run 2.....	18
Figure 12.	Blade Wake Survey: 2/24/94 Run 4.....	18
Figure 13.	Angle Distribution Comparison.....	19
Figure 14.	Probe Static Pressure Distribution.....	21
Figure 15.	Baseline Blade Wake Survey: Run 1.....	24
Figure 16.	Baseline Blade Wake Survey: Run 2 .....	25
Figure 17.	Baseline Blade Wake Survey: Run 3 .....	26
Figure 18.	Baseline Blade Wake Survey: Run 4 .....	27
Figure 19.	Baseline Blade Wake Survey: Run 5 .....	28
Figure A1.	Program "CAL_ACQ".....	33
Figure C1.	Pitch Angle vs. Gamma X = 0.1047.....	39
Figure C2.	Pitch Angle vs. Gamma X = 0.1397.....	39
Figure C3.	Pitch Angle vs. Gamma X = 0.1812 .....	40

<b>Figure C4.</b>	Pitch Angle vs. Gamma	X = 0.2192	.....	40	
<b>Figure C5.</b>	Pitch Angle vs. Gamma	X = 0.2650	.....	41	
<b>Figure C6.</b>	Pitch Angle vs. Gamma	X = 0.3002	.....	41	
<b>Figure C7.</b>	Pitch Angle vs. Gamma	X = 0.3378	.....	42	
<b>Figure C8.</b>	Pitch Angle vs. Gamma	X = 0.3698	.....	42	
<b>Figure C9.</b>	X vs. Beta		.....	43	
<b>Figure D1.</b>	Program	"NEW_READ_ZOC1"	.....	46	
<b>Figure E1.</b>	Fully-Mixed-Out Control Volume		.....	60	
<b>Figure F1.</b>	Run 2	2/24/94	Raw Data	.....	64
<b>Figure F2.</b>	Run 4	2/24/94	Raw Data	.....	66
<b>Figure F3.</b>	Run 5	2/24/94	Raw Data	.....	68

## LIST OF SYMBOLS

$a_0$ - $a_6$	Coefficients of Eq. (5)
$b_0$ - $b_3$	Coefficients of Eq. (6)
$C_p$	Specific heat at constant pressure
$d_s$	Distance of one blade space
$d_1$	Staggered passage width
$M$	Mach number
$P$	Pressure
$P_T$	Stagnation (total) pressure
$P_1$	Probe pressure (center tube)
$P_2$	Probe pressure (side hole-facing down)
$P_3$	Probe pressure (side hole-facing up)
$P_{23}$	Average of $P_2$ and $P_3$
$T_T$	Stagnation temperature
$V$	Velocity
$V_T$	Limiting velocity
$X$	Dimensionless velocity
$B$	Defined by Eq. (3)
$\beta_i$	Flow angle
$\gamma$	Ratio of Specific Heats
$\Gamma$	Defined by Eq. (4)
$\theta$	Flow angle to the probe axis ( and to inlet flow direction)
$\phi$	Pitch angle
$\Phi$	Pitch angle at $X_i$ =constant

$\bar{\omega}$	Mass-averaged loss coefficient
$\omega_{\text{mixed}}$	Mixed-out loss coefficient defined in Appendix E, Eq. (13)

## ACKNOWLEDGEMENTS

I would like to take this opportunity to thank those people who have made my time at NPS such a rewarding experience. Professor Raymond Shreeve has kept me centered on my objectives and taught me not only the principles of turbomachinery, but also the proper method of engineering research. His patience and attention to detail was a positive influence on me. Professor Garth Hobson's enthusiasm and energy provided an outstanding environment for work and learning at the Turbopropulsion Lab. I am grateful to Rick Still and Thad Best for their skill at operating the transonic cascade wind tunnel and free-jet. I would like to thank John Moulton for crafting such an excellent probe tip for use in the transonic cascade traverse system. I am also grateful to Don Harvey and Pat Hickey for their skilled advice in the design of the probe calibration apparatus. Finally, I thank my wife Rachel, whose love, support, and constant encouragement has kept me focused on my goals and the light at the end of this tunnel.



## I. INTRODUCTION

The requirement to achieve higher compressor ratios in the fan stages of military and civilian engines has led to increasing supersonic relative inlet Mach numbers. The higher Mach numbers lead to stronger shock waves forming in the rotor passages near the blade leading edge. These strong shocks interact with the turbulent boundary layer on the suction side of each blade to produce the flow field depicted in Figure 1.

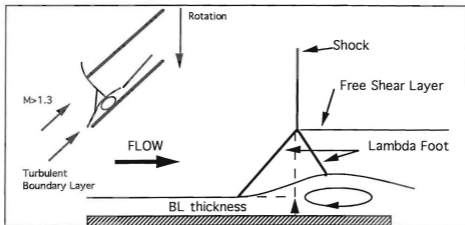


Figure 1. Shock-Boundary Layer Interaction

The shock-boundary layer interaction is characterized by the lambda foot and a local region of reversed flow. The strong shock-boundary layer interaction adversely effects the total pressure ratio and flow turning angle of the compressor blade row. A concept for alleviating the shock-induced boundary layer separation is the use of low-profile vortex generators affixed to the suction surface of the rotor blading, some distance ahead of where the shock impinges.



Vortex generator devices alleviate the shock interaction by energizing the low momentum region of the boundary layer with relative near-freestream flow via streamwise vortices. The vortex generators reduce the relative total pressure loss in the rotor by reducing the size of the local separation and also improve the flow turning angle toward that required by the design. In the present study, 6-5-1 "Triangular Plow Vortex Generators", depicted in Figure 2 and described by McCormick [Ref. 1] and United Technologies Research Center [Ref. 2], were to be used in a model transonic Fan-Blade cascade to quantify their effect on the total pressure losses and flow turning angle and thereby assess the potential benefits of this technique.

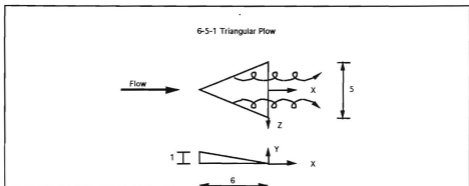


Figure 2. Low-Profile Vortex Generator

The model cascade apparatus was first assembled and operated by Collins [Ref. 3]. First successful static pressure measurements were made by Golden [Ref. 4] and impact probe traverse measurements by Myre [Ref. 5]. Tapp [Ref. 6] showed that repeatable periodic conditions could be achieved at the design flow angle using wall bleed. In the present study, a three-port traversing pneumatic probe was designed, calibrated, and used to measure dimensionless velocity and

flow angle over the outlet of a blade passage. These values were used to calculate a fully-mixed-out condition, and hence the total pressure loss and flow turning angle. A follow-on study will apply the techniques reported here to assess the effects of vortex generators. In the present document, Chapter II describes the design and calibration of the three-port probe and the transonic fan-blade cascade model. Chapter III describes the experimental program and test results. Chapter IV includes the conclusions and recommendations for further work.

## II. EXPERIMENTAL DEVELOPMENTS

### A. PROBE DESIGN

To measure Mach number and flow angle behind the model fan-blade passage required a probe that was sensitive to only Mach number and pitch angle, since the yaw angle was zero at mid-span. It was desirable (though not necessary) that the arrangement of sensors would result in two pressure coefficients such that one was insensitive to changes in pitch angle at constant Mach number and the other insensitive to changes in Mach number at constant pitch angle. AGARD-AG-207 [Ref. 7] reported probe designs that had such characteristics, which guided the present design shown in Figure 3.

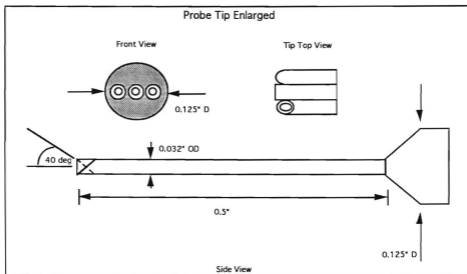


Figure 3. Probe Tip Enlarged

Additionally, the probe was required to measure velocities in a shear layer as it traversed through the fan-blade wake, which required that the ports all lie in the same plane. Myre [Ref. 5] developed a traversing impact probe system for use in the present experiment with the ability to accommodate different probe tips. The present probe was designed to fit the existing probe holder and traverse system for use with the current data acquisition system hardware and software reported by Myre [Ref. 5]. A three-port pneumatic probe was chosen using 0.032" OD stainless steel tubing. The center port was cut normal to the tunnel axis with the outer two ports shaved to an angle of approximately forty degrees in opposite directions.

## **B. PROBE CALIBRATION**

The probe calibration was carried out in the Turbopropulsion Laboratory's free-jet calibration apparatus which is shown in Figure 4. The probe holder assembly is described by Myre [Ref. 5] and depicted in Figure 5. The nozzle of the free-jet was 4.25 inches in diameter and was fed by an Allis-Chalmers compressor delivering air at a pressure of up to three atmospheres. The Mach number range of the free-jet, which exhausted to atmosphere, was from 0 to 0.9. The probe holder was attached to an apparatus mounted to the free-jet nozzle which allowed the operator to accurately set and vary the pitch angle of the probe, as required for the calibration. A Prandtl probe was installed 0.5 inches from the jet centerline to provide redundancy in the measurement of Mach number.

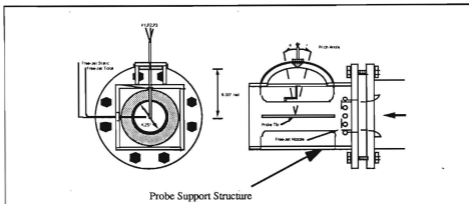


Figure 4. Free-Jet Calibration Apparatus

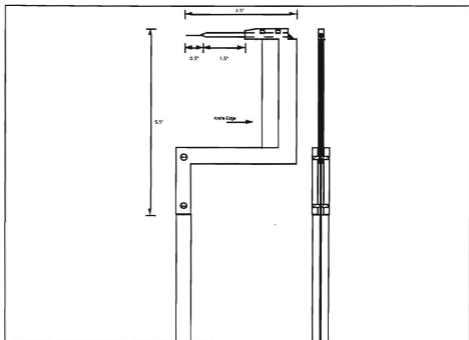


Figure 5. Probe Holder Assembly

## 1. Data Acquisition System

The pressure measurements of the probe (3), free-jet static pressure (atmospheric), and free-jet total pressure were acquired using a +/- 50 psid Scanivalve transducer controlled by a Hewlett-Packard 9000-300 series computer. The HP 9000 computer sent commands via a HG-78K Scanivalve controller developed by Geopfarth [Ref. 8] to the Scanivalve. It in turn sent the measured voltage of the transducer to a HP 3456A digital voltmeter, which was read by the computer. The voltages were recorded and converted to psia in an HP BASIC data acquisition program, "CAL\_ACQ", listed in Appendix A. Golden [Ref. 4] describes in detail the use of the data acquisition system.

## 2. Program of Measurements

The impact probe and probe assembly were removed from the transonic cascade and the new three-port probe design was installed. The new probe and probe holder assembly were mounted in the free-jet calibration apparatus. The probe was leveled in its mount, then securely fastened in place. The probe tip was located at the center of the free-jet, which has been shown to have a uniform velocity profile by Neuhoff [Ref. 9]. The free-jet static and total pressures were used to calculate the jet Mach number and limiting velocity using isentropic gas relations with the ratio of specific heats equal to 1.4. The relation between total (stagnation) pressure, static pressure, and dimensionless velocity is

$$\frac{P}{P_T} = (1 - X^2)^{\frac{\gamma}{\gamma-1}} \quad (1)$$

where

$$X = \frac{V}{\sqrt{2C_p T_T}}$$

The Mach number was held stable while 12 pitch angles were set in turn and pressure data were recorded. The Mach number was varied in steps of 0.1 from  $M = 0.2$  to  $0.9$ , giving a total of 96 calibration data points. In the calculation of dimensionless velocity the center port pressure measurement was taken to be total pressure since it was always in the center of the flow and always read slightly higher than the Prandtl probe total pressure. The static pressure was taken to be atmospheric, which was consistent with the Prandtl probe measurements. The raw data from the calibration are listed in Table B1 and Table B2 of Appendix B.

### 3. Probe Characteristics

The derivation of the probe pressure coefficients followed the work of Neuhoff [Ref. 9]. If  $P_1$  is the pressure at the center port and  $P_2$  and  $P_3$  are the pressures of the two side ports, we define the average of  $P_2$  and  $P_3$  as  $P_{23}$ , where

$$P_{23} = \frac{P_2 + P_3}{2} \quad (2)$$

and the two pressure coefficients used to represent the calibration of the probe in terms of Mach number and pitch angle are

$$\text{Beta} = B = \frac{P_1 - P_{23}}{P_1} \quad (3)$$

and

$$\text{Gamma} = \Gamma = \frac{P_2 - P_3}{P_1 - P_{23}} \quad (4)$$

The measured characteristics of the probe in terms of Beta and Gamma are shown in Figures 6 and 7 respectively. The Mach-sensitive coefficient Beta

was found to be relatively insensitive to changes in pitch angle over the entire Mach range. The pitch sensitive coefficient Gamma was found to be relatively insensitive to changes in Mach number over the range of pitch angles.

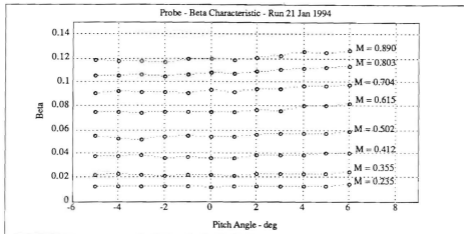


Figure 6. Beta Characteristic

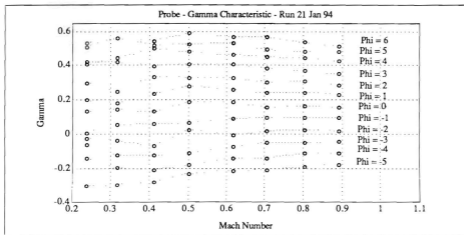


Figure 7. Gamma Characteristic



The insensitivity of Beta to pitch angle allowed the Mach number and dimensionless velocity, X, to be approximated by a polynomial in terms of Beta only. The polynomial for X as a function of Beta was derived utilizing the least-squares method, using an average value of Beta over the range of pitch angle. The program MATLAB was used to determine this polynomial and a choice of a sixth-order polynomial was found to give the least error in X over the calibration range. The polynomial is shown as Equation 5, with the values of the coefficients listed below. The sixth-order polynomial is shown and plotted vs. the actual data points in Appendix C.

$$\begin{aligned}
 X &= a_6B^6 + a_5B^5 + a_4B^4 + a_3B^3 + a_2B^2 + a_1B + a_0 \\
 a_6 &= -1733913.202 \\
 a_5 &= +679216.632 \\
 a_4 &= -104416.881 \\
 a_3 &= +8119.488 \\
 a_2 &= -344.912 \\
 a_1 &= +10.120 \\
 a_0 &= +0.018
 \end{aligned}
 \tag{5}$$

A third-order polynomial for pitch angle was derived in terms of Gamma at each average dimensionless velocity using the least-squares method and the MATLAB software. The polynomial has the form of Equation 6 with the coefficients summarized in Table 1. The third-order polynomials of pitch angle in terms of Gamma are plotted vs. the actual data points in Appendix C.

$$\Phi_i = b_3\Gamma^3 + b_2\Gamma^2 + b_1\Gamma + b_0
 \tag{6}$$

where

$$X_i = \text{constant}$$

**TABLE 1. PROBE CALIBRATION COEFFICIENTS**

	$X_i$	$b_3$	$b_2$	$b_1$	$b_0$
$\Phi_1$	0.1047	-0.815	3.584	12.251	-1.841
$\Phi_2$	0.1397	0.156	0.412	12.112	-1.548
$\Phi_3$	0.1812	19.817	-5.526	9.996	-1.461
$\Phi_4$	0.2192	13.149	-3.288	11.104	-1.973
$\Phi_5$	0.2650	15.897	-5.546	12.155	-2.072
$\Phi_6$	0.3002	3.438	0.520	13.270	-2.268
$\Phi_7$	0.3378	11.242	-2.607	13.736	-2.349
$\Phi_8$	0.3698	11.968	-3.634	14.607	-2.347

#### 4. Application of the Calibration

The method of application of the calibration was first to take the measured probe pressures and determine the coefficients Beta and Gamma. From the Beta coefficient, the dimensionless velocity could be determined immediately using the sixth-order polynomial. With the dimensionless velocity known, the third-order polynomials of pitch angle in terms of Gamma could be calculated for the curves associated with the values of the dimensionless velocity above and below the calculated dimensionless velocity. An interpolation scheme given by Nakamura [Ref. 10] was then used to interpolate for the pitch angle at that known velocity and value of Gamma. The results of applying the calibration method to the actual data is given in Appendix C. Over the entire range of the calibration the uncertainty in dimensionless velocity was found to be +/- two percent with a confidence of 70 percent. The pitch angle uncertainty was found

to be +/- 0.2 degrees with a confidence of 76 percent. Above a dimensionless velocity value of 0.18, the confidence level increased due to the improved resolution of the data acquisition system at the higher velocities. Above this velocity, where most of the cascade measurements were to be taken, the confidence in determining dimensionless velocity and pitch angle accurately rose to 73 percent and 96 percent respectively. A Kline and McClintock uncertainty analysis [Ref. 11] was performed and at the lower velocities,  $X < 0.18$ , the uncertainty in Beta and Gamma was much higher than at the higher velocities. This explains why the calibration scheme is more accurate at the higher velocities and why the Gamma characteristic behaves poorly at lower velocities. The calibration application program, written in Hewlett-Packard Basic is listed in the data reduction program "NEW\_READ\_ZOC1", in Appendix D.

## C. TRANSONIC CASCADE MODEL AND DATA ACQUISITION

### 1. Transonic Cascade Model

The transonic cascade model attempts to simulate the relative flow at  $M=1.4$  on a stream surface through a Navy developmental transonic fan. The current model has been shown by Golden [Ref. 4] to be closely two dimensional with the placement of the shock structure set manually using an in-line shadowgraph while adjusting back pressure and bleed valves. The vertically-traversing probe assembly designed by Myre [Ref. 5] was used with the new probe design. Myre also describes the use of the traversing system [Ref. 5]. The wind tunnel facility is shown schematically in Figure 8. The transonic cascade model test section is shown in Figure 9. The model simulation is of the flow through two passages of the transonic blading geometry which is shown in Figure 10. In the cascade simulation, the design pressure ratio and shock

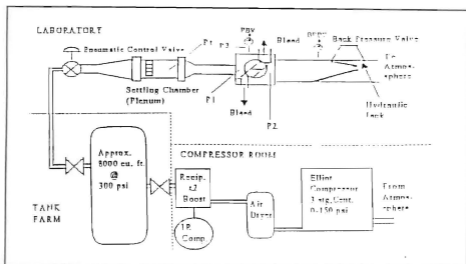


Figure 8. Wind Tunnel Facility

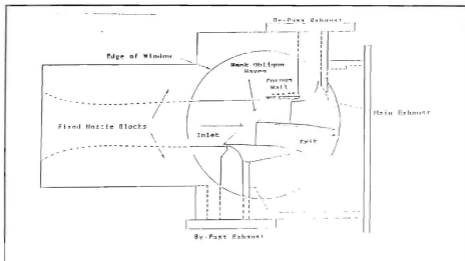


Figure 9. Transonic Cascade Model Test Section

structure at the design incidence were set using the "Back-Pressure Valve (BPV)". A "Back-Pressure Bleed Valve (BPBV)" was used for fine adjustments in setting the proper shock structure (Figure 8).

## 2. Data Acquisition System

The data acquisition system utilized in the present study was used previously by Tapp [Ref. 6]. One +/- 50 psid ZOC-14 enclosure was used to record the three pressures of the traversing probe. Plenum and wall reference pressures were also recorded. The data acquisition program "NEW\_SCAN\_ZOC" [Ref. 5] was modified slightly to allow the probe-traverse mechanism to increment in smaller steps through the wake, in order to improve the spatial resolution. To change the increment step size required a change in only a single line of code. The initial starting point of the probe-traverse assembly was also changed by a single entry.

The data reduction program "READ\_ZOC2" [Ref. 5] was modified for use in the current study and renamed "NEW\_READ\_ZOC1". The principal change was the application of the routine to return dimensionless velocity and flow angle from the three pressure measurements. The calculation of the fully-mixed-out condition was also calculated in the program. The program is listed in Appendix D and the calculation of the fully-mixed-out condition is summarized in Appendix E. A complete derivation of the method for calculating the fully-mixed-out dimensionless velocity, flow angle, and total pressure is contained in Reference 12.

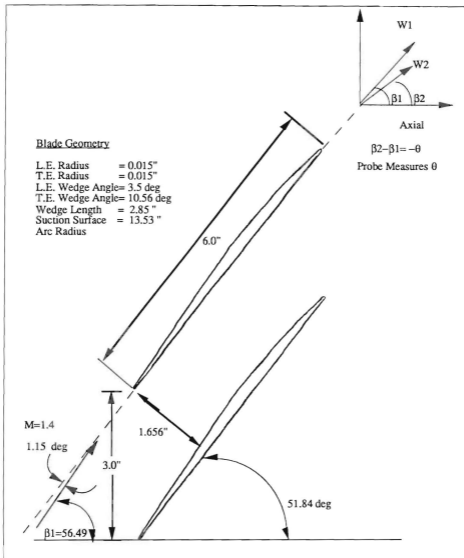


Figure 10. Cascade Blading Geometry

### III. EXPERIMENTAL PROGRAM, RESULTS AND DISCUSSION

#### A. EXPERIMENTAL PROGRAM

The experimental program consisted of a series of initial runs with equal-increment probe traverses through the center blade wake. These tests were used to refine the operation of the pressure valves in setting the shock structure, to become familiar with the data acquisition procedures, and to verify the revised coding of the data reduction program "NEW\_READ\_ZOC1". Repeatability tests were then conducted to verify that the impact probe measurements compared with previous results reported by Myre [Ref. 5] and Tapp [Ref. 6]. Once these tests were completed the number of data points in the blade wake was increased to provide better resolution through the wake. These tests were used to examine probe-derived static pressure and angle distributions through the wake. Finally, five tests were conducted to provide baseline data and to establish the fully-mixed-out condition for use in studies to assess the effect of vortex generating devices. In all the tests, the shocks in the upper and lower passages were repeatedly set to the expected on-design position, using the following procedure:

- 1. The tunnel was allowed to become steady at a plenum pressure of 33 psig.
- 2. While carefully monitoring the shadowgraph, the BPV was closed by four smooth movements of the hydraulic jack handle.

- 3. A fifth movement of the jack handle (done smoothly) was stopped just as the lower passage shock was in position at a mark on the tunnel side plate (visible in the shadowgraph).
- 4. The BPBV was closed until the upper passage shock was in the corresponding position. Its position was monitored visually throughout the data acquisition during the probe traverse.

## B. REPEATABILITY TESTS

These tests were run to compare the mass-averaged loss coefficient results obtained with the new probe and those obtained by Myre [Ref. 5] and Tapp [Ref. 6], using an equal-increment traverse procedure, across a distance of two inches. The probe tip was approximately 1 1/8 inches downstream of the trailing edge of the middle blade with the probe starting its traverse 1.0 inch above the level of the blade trailing edge. Figures 11 and 12 show the blade-wake pressures vs. vertical position during the traverse. Table 2 summarizes the results of tests in which tunnel supply conditions were held reasonably constant.

TABLE 2. REPEATABILITY TESTS: 2/24/94 RUN 2 AND RUN 4

Run #	Patm (psia)	P2/P1	T <sub>T</sub> (R)	$\sigma$
2	14.72	2.11	514.5	0.0842
4	14.715	2.09	513.0	0.0847

The raw pressure data for the complete test program are listed in Appendix F. The mass-averaged losses compared well (to within three percent) with previous results [Ref. 5 & 6] with similar tunnel conditions. The data confirmed that the



probe, data acquisition system, and data reduction process were operating properly.

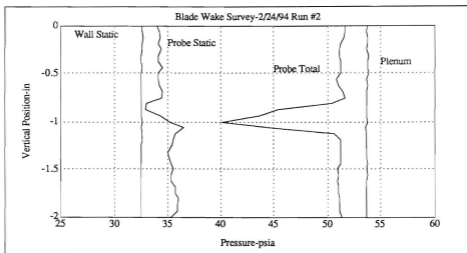


Figure 11. Blade Wake Survey: 2/24/94 Run 2

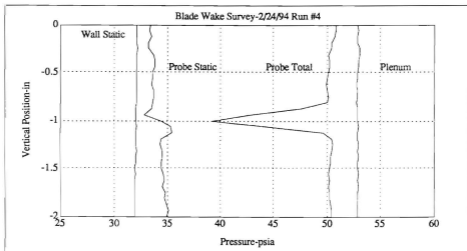
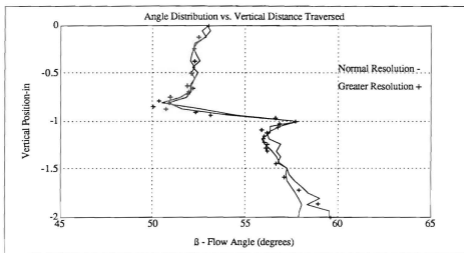


Figure 12. Blade Wake Survey: 2/24/94 Run 4

Probe-derived static pressure profiles are shown in Figures 11 and 12. It is seen that the static pressure on the suction side of the blade was lower than that on the pressure side, implying a higher velocity in that portion of the upper passage. A change in static pressure through the wake can clearly be seen. Both runs show a reasonably periodic condition in the cascade model based only on the measured total pressure.

### C. TURNING ANGLE DISTRIBUTION

Figure 13 shows the distribution of the flow angle derived from probe measurements in three similar tests.



**Figure 13.** Angle Distribution Comparison

Figure 13 contains data from Runs 2, 4, and 5 of 2/24/94. As presented previously, Runs 2 and 4 were equal-increment surveys for a two inch traverse. Run 5 was a survey which stepped 0.03125 inches per increment through 22 points just prior to, and through the blade wake, providing better spatial

resolution. The start and end points remained the same for all three runs. The data are seen to be similar for all runs. The angle distribution is characterized by increased values of outlet flow angle ( $\beta_2$ ) from the upper portion of the lower passage (less turning). The value of  $\beta_2$  from the upper passage approaches that of the design value of 50 degrees. The flow angle behaves similarly to the static pressure through the turbulent blade wake. Without further measurements, the differences in flow angle and dimensionless velocity cannot be explained definitively. The higher turning angle in the upper passage and lower turning angle in the lower passage is most probably the result of the significant differences in the wakes of the center and lower blades. The center blade is a true blade wake, the lower blade wake is a mixing layer, with entrainment from the test section cavity. In viewing the probe distributions, it should be remembered that the traverse was not parallel to the blade trailing edges so that the lower part of the traverse is further downstream of the blading than is the upper part. The data do show that the angle distributions through the passages were repeatable.

#### **D. PROBE STATIC PRESSURE DISTRIBUTION**

Figure 14 shows a comparison of probe-derived static pressure for the same tests as in Figure 13. The static pressure distributions all have the same form, and were reasonably repeatable. The improved resolution blade-wake surveys clearly show a steep decline in static pressure as the probe entered the blade wake, then a sharp rise through the wake. The static pressure rises slightly again on the pressure side of the blade wake, then stabilizes at a value above that of the upper passage.

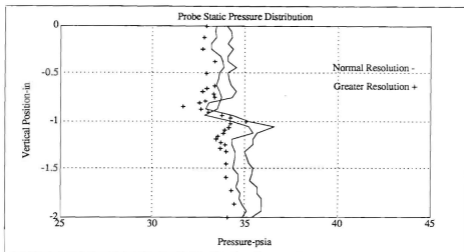


Figure 14. Probe Static Pressure Distribution

#### E. MODEL BASELINE MEASUREMENTS

The model baseline measurements were made using a survey distance of 1.656 inches (equal to the staggered-passage width, Figure 10) with the probe starting position located 0.75 inches above the level of the middle blade trailing edge. ZOC 1 was used for the probe surveys with the measured pressures and their associated ports listed in Table 3. Table 4 lists the probe positions relative to the starting point with point 1 being the beginning of the traverse above the middle blade. Five runs were made to determine the flow profiles and the baseline loss coefficient using the fully-mixed-out conditions calculated as shown in Appendix E. Table 5 lists the tunnel conditions for the five runs and Table 6 lists the results of the fully-mixed-out calculations. Figures 15 through 19 show the blade wake survey results output by the data reduction program "NEW\_READ\_ZOC1".

**TABLE 3. MEASURED PRESSURES AND PORTS ASSIGNED**

Measured Pressure psia	Port Assigned
Atmospheric	1
P1	32
P2	24
P3	25
Upstream Static	29
Downstream Static	30
Plenum	31

**TABLE 4. PROBE TRAVERSE POSITON**

Point	Relative Position-in	Point	Relative Position-in	Point	Relative Position-in
1	0	12	0.50	23	0.84375
2	0.0625	13	0.53125	24	0.875
3	0.125	14	0.5625	25	0.90625
4	0.1875	15	0.59375	26	0.9375
5	0.25	16	0.625	27	0.96875
6	0.3125	17	0.65625	28	1.00
7	0.34375	18	0.6875	29	1.13125
8	0.375	19	0.71875	30	1.2625
9	0.40625	20	0.75	31	1.39375
10	0.4375	21	0.78125	32	1.525
11	0.46875	22	0.8125	33	1.65625

**TABLE 5. BASELINE TUNNEL CONDITIONS**

Run #	Upstream Static-psia	P2/P1	T <sub>T</sub> (R)	Plenum- psia	Mass Flux Integral
1	15.279	2.09	518.7	48.45	0.9143
2	15.128	2.08	519.7	47.94	0.9140
3	15.379	2.08	518.2	48.76	0.9196
4	15.043	2.07	518.2	47.75	0.9218
5	15.047	2.09	517.7	47.65	0.9227

**TABLE 6. BASELINE FULLY-MIXED-OUT CONDITIONS**

Run #	X <sub>3</sub>	Pt <sub>3</sub> - psia	β <sub>3</sub> -deg	$\sigma_{mixed}$
1	0.3115	40.73	55.14	0.2328
2	0.3118	40.31	55.15	0.2327
3	0.3100	40.58	54.73	0.2450
4	0.3159	39.76	55.05	0.2443
5	0.3143	39.73	54.92	0.2432
AVERAGE	0.3127	40.22	55.00	0.2396

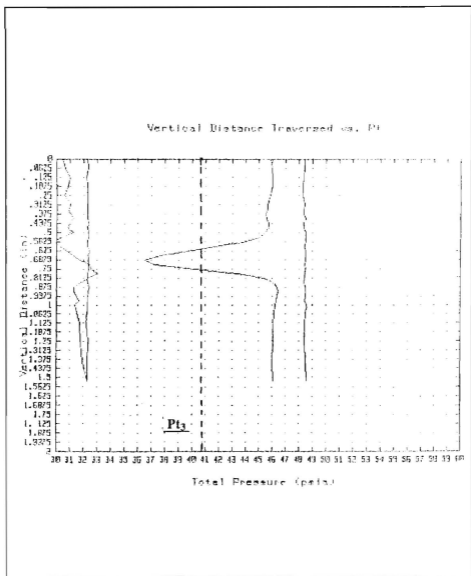


Figure 15. Baseline Blade Wake Survey: Run 1

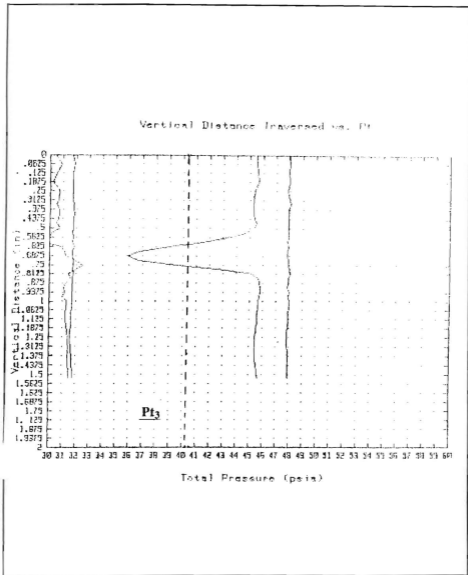


Figure 16. Baseline Blade Wake Survey: Run 2



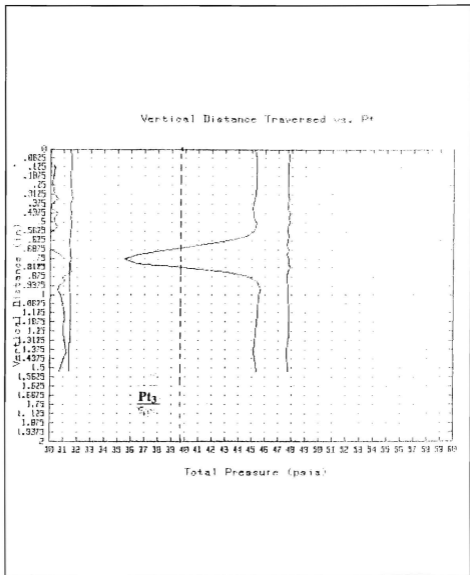


Figure 17. Baseline Blade Wake Survey: Run 3

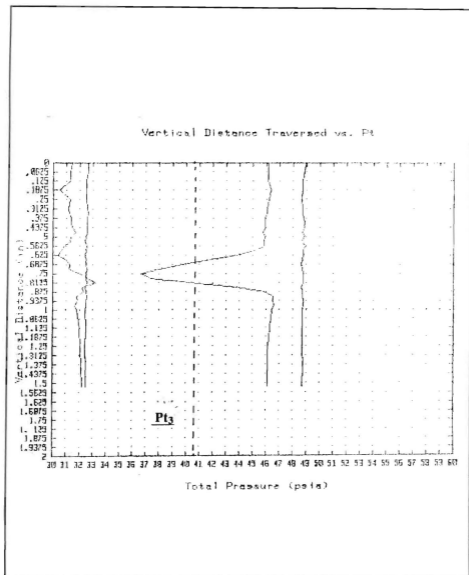


Figure 18. Baseline Blade Wake Survey: Run 4

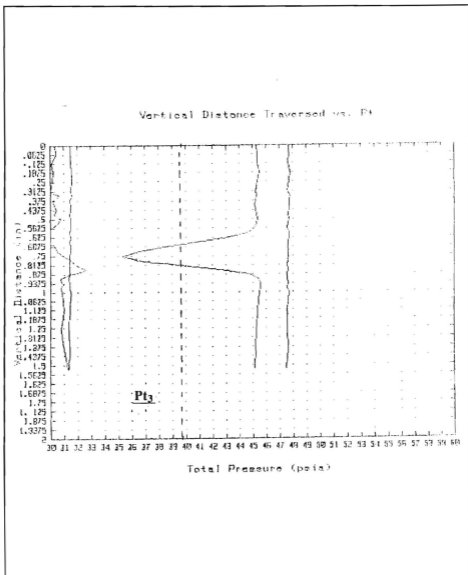


Figure 19. Baseline Blade Wake Survey: Run 5

In all cases, the calculated fully-mixed-out total pressure ( $P_{t3}$ ) was repeatable and qualitatively showed a low but not unreasonable value when compared to probe-measured total pressure distribution, which was reasonably periodic. The probe-derived static pressure distributions were also repeatable, and followed the trends of the previously discussed results. The calculated fully-mixed-out loss coefficient was more than twice the mass-averaged loss coefficient as presented in Table 2. The fully-mixed-out calculation subprogram in "NEW\_READ\_ZOC1" was verified by programming a known test case used by Armstrong [Ref. 12]. It is noted that the test case was at low Mach number, rather than the high subsonic range of the present measurements. However, it is also noted that Armstrong also reported that much higher values were obtained for the fully-mixed-out loss coefficient than for the mass-averaged loss coefficient, when reducing cascade-flow survey data.

#### IV. CONCLUSIONS AND RECOMMENDATIONS

In the present study, the velocity and flow angle distributions, and the fully-mixed-out losses due to the shock-boundary layer interaction in the transonic fan-blade cascade model, were measured at the design incidence angle. The measured flow field and flow losses provide baseline values for planned measurements with low-profile vortex generator devices installed. The fully-mixed-out loss values were more than twice the mass-averaged loss values reported by Myre [Ref. 5] and Tapp [Ref. 6] and repeated in the present study. The measurements of pressure and flow angle distributions were repeatable. The three-port probe, designed for the present study, gave excellent results in measurements of static pressure, dimensionless velocity and flow angle, at velocities greater than  $M = 0.4$ .

The following specific conclusions were drawn:

- Shock placement using the Back Pressure Valve (BPV), Back Pressure Bleed Valve (BPBV), Porous Bleed Valve (PBV), and in-line shadowgraph system was quick, and gave repeatable results.
- The calculated fully-mixed-out flow losses were significantly higher than mass-averaged results. This may have been due to the probe not traversing parallel to the trailing edge, but a more detailed analysis of how this would effect the calculation needs to be made.
- The probe-derived static pressure in the flow from the suction side of the center blade was lower than that from the pressure side, indicating a higher velocity in the upper passage.

- Angle distributions obtained in the surveys were repeatable and showed less flow turning from the pressure side of the middle blade than from the suction side.
- The probe in its present location, traversing normal to inlet velocity, could not determine the degree of periodicity in the two-passage fan-blade model.
- The probe design had excellent characteristics at medium to high Mach numbers and had the ability to measure accurately in the wake shear layers. Measurements of static pressure and flow angle through the blade wake were consistent with previous experience at lower Mach numbers [Ref. 13].

The following recommendations are made concerning the present pilot and follow-on research program:

- Use the same probe design but increase the range of the angle calibration from -6 degrees to +12 degrees.
- Design and build an apparatus to calibrate the probe in the probe holder while still attached to the motor-controller assembly and utilizing the ZOC system for data acquisition.
- Make more measurements with the current system and validate the calculation of the fully-mixed-out loss .
- Install the 6-5-1 Triangular Plow Vortex Generator Devices and compare the loss measurements and the flow field to the baseline results.

- Once these pilot experiments are complete, proceed to a larger apparatus in which Mach number and cascade geometry can be varied. In the larger apparatus, design the traverse to be parallel to the blade trailing edge.
- The larger apparatus should incorporate three blades to improve the ability to simulate periodicity.

## APPENDIX A. PROGRAM "CAL\_ACQ"

```

100
101
102
103
104
105
106
107
108
109
110
111
112
113
114
115
116
117
118
119
120
121
122
123
124
125
126
127
128
129
130
131
132
133
134
135
136
137
138
139
140
141
142
143
144
145
146
147
148
149
150
151
152
153
154
155
156
157
158
159
160
161
162
163
164
165
166
167
168
169
170
171
172
173
174
175
176
177
178
179
180
181
182
183
184
185
186
187
188
189
190
191
192
193
194
195
196
197
198
199
200
201
202
203
204
205
206
207
208
209
210
211
212
213
214
215
216
217
218
219
220
221
222
223
224
225
226
227
228
229
230
231
232
233
234
235
236
237
238
239
240
241
242
243
244
245
246
247
248
249
250
251
252
253
254
255
256
257
258
259
260
261
262
263
264
265
266
267
268
269
270
271
272
273
274
275
276
277
278
279
280
281
282
283
284
285
286
287
288
289
290
291
292
293
294
295
296
297
298
299
300
301
302
303
304
305
306
307
308
309
310
311
312
313
314
315
316
317
318
319
320
321
322
323
324
325
326
327
328
329
330
331
332
333
334
335
336
337
338
339
340
341
342
343
344
345
346
347
348
349
350
351
352
353
354
355
356
357
358
359
360
361
362
363
364
365
366
367
368
369
370
371
372
373
374
375
376
377
378
379
380
381
382
383
384
385
386
387
388
389
390
391
392
393
394
395
396
397
398
399
400
401
402
403
404
405
406
407
408
409
410
411
412
413
414
415
416
417
418
419
420
421
422
423
424
425
426
427
428
429
430
431
432
433
434
435
436
437
438
439
440
441
442
443
444
445
446
447
448
449
450
451
452
453
454
455
456
457
458
459
460
461
462
463
464
465
466
467
468
469
470
471
472
473
474
475
476
477
478
479
480
481
482
483
484
485
486
487
488
489
490
491
492
493
494
495
496
497
498
499
500
501
502
503
504
505
506
507
508
509
510
511
512
513
514
515
516
517
518
519
520
521
522
523
524
525
526
527
528
529
530
531
532
533
534
535
536
537
538
539
540
541
542
543
544
545
546
547
548
549
550
551
552
553
554
555
556
557
558
559
560
561
562
563
564
565
566
567
568
569
570
571
572
573
574
575
576
577
578
579
580
581
582
583
584
585
586
587
588
589
590
591
592
593
594
595
596
597
598
599
600
601
602
603
604
605
606
607
608
609
610
611
612
613
614
615
616
617
618
619
620
621
622
623
624
625
626
627
628
629
630
631
632
633
634
635
636
637
638
639
640
641
642
643
644
645
646
647
648
649
650
651
652
653
654
655
656
657
658
659
660
661
662
663
664
665
666
667
668
669
670
671
672
673
674
675
676
677
678
679
680
681
682
683
684
685
686
687
688
689
690
691
692
693
694
695
696
697
698
699
700
701
702
703
704
705
706
707
708
709
710
711
712
713
714
715
716
717
718
719
720
721
722
723
724
725
726
727
728
729
730
731
732
733
734
735
736
737
738
739
740
741
742
743
744
745
746
747
748
749
750
751
752
753
754
755
756
757
758
759
760
761
762
763
764
765
766
767
768
769
770
771
772
773
774
775
776
777
778
779
780
781
782
783
784
785
786
787
788
789
790
791
792
793
794
795
796
797
798
799
800
801
802
803
804
805
806
807
808
809
810
811
812
813
814
815
816
817
818
819
820
821
822
823
824
825
826
827
828
829
830
831
832
833
834
835
836
837
838
839
840
841
842
843
844
845
846
847
848
849
850
851
852
853
854
855
856
857
858
859
860
861
862
863
864
865
866
867
868
869
870
871
872
873
874
875
876
877
878
879
880
881
882
883
884
885
886
887
888
889
890
891
892
893
894
895
896
897
898
899
900
901
902
903
904
905
906
907
908
909
910
911
912
913
914
915
916
917
918
919
920
921
922
923
924
925
926
927
928
929
930
931
932
933
934
935
936
937
938
939
940
941
942
943
944
945
946
947
948
949
950
951
952
953
954
955
956
957
958
959
960
961
962
963
964
965
966
967
968
969
970
971
972
973
974
975
976
977
978
979
980
981
982
983
984
985
986
987
988
989
990
991
992
993
994
995
996
997
998
999
1000

```

Figure A1. Program "CAL\_ACQ"





```

11000  * *****
11010  * 11 051 0000
11020  * *****
11030  * *****
11040  * *****
11050  * *****
11060  * *****
11070  * *****
11080  * *****
11090  * *****
11100  * *****
11110  * *****
11120  * *****
11130  * *****
11140  * *****
11150  * *****
11160  * *****
11170  * *****
11180  * *****
11190  * *****
11200  * *****
11210  * *****
11220  * *****
11230  * *****
11240  * *****
11250  * *****
11260  * *****
11270  * *****
11280  * *****
11290  * *****
11300  * *****
11310  * *****
11320  * *****
11330  * *****
11340  * *****
11350  * *****
11360  * *****
11370  * *****
11380  * *****
11390  * *****
11400  * *****
11410  * *****
11420  * *****
11430  * *****
11440  * *****
11450  * *****
11460  * *****
11470  * *****
11480  * *****
11490  * *****
11500  * *****
11510  * *****
11520  * *****
11530  * *****

```

Figure A1. (cont) Program "CAL\_ACQ"



## APPENDIX B. PROBE CALIBRATION RAW DATA

**TABLE B1. PROBE CALIBRATION RAW DATA** X = 0.10 - 0.22

ANGLE (deg)	P1 (psia)	P2 (psia)	P3 (psia)	PSTAT (psia)	PTOT (psia)	P2 & P3 avg	X	GAMMA	BETA
-5	15.4089	15.1831	15.2424	14.8421	15.3847	15.21275	0.1030245	0.30543394	0.0126015
-4	15.4051	15.201	15.2288	14.8217	15.3559	15.2139	0.10473862	0.3148224	0.0124147
-3	15.412	15.2172	15.228	14.8271	15.365	15.2228	0.10484825	0.05702218	0.01282913
-2	15.413	15.2133	15.2178	14.83	15.3644	15.21545	0.104673	0.02176644	0.0128171
-1	15.4082	15.2139	15.212	14.8279	15.3684	15.21295	0.10453122	0.00988153	0.0127359
0	15.4052	15.2353	15.2104	14.825	15.3591	15.22285	0.10410681	0.13602841	0.0118831
1	15.4063	15.24	15.2029	14.8277	15.3615	15.22145	0.10428477	0.20070321	0.01168834
2	15.422	15.2527	15.1931	14.8292	15.3692	15.2229	0.1055302	0.2993708	0.01291013
3	15.4132	15.2574	15.174	14.8223	15.3688	15.2157	0.10538908	0.42227848	0.01281369
4	15.4128	15.2508	15.1687	14.8258	15.3484	15.2098	0.10503718	0.40492611	0.01317087
5	15.4177	15.2603	15.1581	14.8252	15.3711	15.2182	0.10498581	0.5048938	0.01313937
6	15.4224	15.2587	15.141	14.8241	15.359	15.19885	0.1080242	0.52868992	0.01443031
-5	15.8937	15.4878	15.5392	14.8281	15.8155	15.5398	0.14025233	0.29499859	0.02225888
-4	15.9020	15.5044	15.5272	14.8272	15.8143	15.5418	0.14079287	0.19574233	0.02274342
-3	15.8948	15.528	15.5892	14.8289	15.826	15.5488	0.14012025	0.11907514	0.0217684
-2	15.8884	15.5387	15.5504	14.8363	15.8079	15.54455	0.13922888	0.03402647	0.02164157
-1	15.9001	15.5428	15.544	14.8282	15.8158	15.5533	0.14051288	0.05363322	0.02181118
0	15.9038	15.5784	15.5248	14.8319	15.8188	15.5505	0.14048959	0.14681781	0.02221482
1	15.8893	15.5801	15.5177	14.8373	15.817	15.5489	0.13921786	0.18331175	0.02149322
2	15.8848	15.5785	15.4889	14.842	15.8168	15.5327	0.13925374	0.25288985	0.02287818
3	15.902	15.6135	15.4981	14.8454	15.8082	15.5383	0.13947239	0.42220299	0.02299711
4	15.9012	15.6104	15.4453	14.8434	15.8202	15.52785	0.13959575	0.44212194	0.02347838
5	15.8893	15.624	15.4178	14.8403	15.8314	15.5009	0.13887836	0.5597177	0.0218541
6	15.9048	15.6245	15.4049	14.8523	16.5731	15.5147	0.13916955	0.96322134	0.02451492
-5	18.7033	18.9884	18.8823	14.8523	18.5731	18.07435	0.18188117	0.27867247	0.03765484
-4	18.7028	18.9078	18.7383	14.8479	18.5051	18.07195	0.1817832	0.20472441	0.03784253
-3	18.7148	18.9353	18.7104	14.8482	18.5912	18.07285	0.18238386	0.11702738	0.03838453
-2	18.6888	18.984	18.7058	14.852	18.5889	18.0849	0.18097829	0.08030857	0.03813974
-1	18.6889	18.9893	18.9517	14.8503	18.5858	18.0705	0.18110881	0.08080207	0.037054527
0	18.6883	18.7223	18.9417	14.8521	18.5806	18.082	0.18098687	0.13253748	0.03833284
1	18.6791	18.7487	18.9074	14.8482	18.5721	18.07855	0.18078623	0.23684848	0.03808814
2	18.6849	18.7883	18.9488	14.8534	18.564	18.05805	0.18122177	0.33995448	0.03814839
3	18.6901	18.7811	18.9271	14.853	18.5387	18.0541	0.18102295	0.38937107	0.03810842
4	18.6888	18.201	18.8783	14.8537	18.5511	18.03885	0.18082878	0.48880207	0.03877085
5	18.7041	18.2085	18.885	14.8534	18.5777	18.03925	0.18184617	0.51849298	0.03888182
6	18.7018	18.2124	18.8461	14.8582	18.5701	18.02025	0.18128133	0.54410533	0.04025862
-5	17.8875	18.0024	18.8294	14.8895	17.4869	18.7195	0.21948894	0.22848308	0.05518011
-4	17.8882	18.0495	18.8131	14.8781	17.508	18.7313	0.21869088	0.17578167	0.05268505
-3	17.8384	18.0728	18.7724	14.8804	17.5167	18.7226	0.21852902	0.1089954	0.0518133
-2	17.8874	18.7212	18.8948	14.8652	17.4827	18.708	0.21941922	0.0275132	0.05430341
-1	17.8858	18.742	18.8751	14.8664	17.4886	18.70855	0.22001339	0.08845741	0.05529619
0	17.8847	18.8048	18.8248	14.8888	17.5487	18.7148	0.2192374	0.18949303	0.0537391
1	17.8849	18.8319	18.8578	14.8704	17.5813	18.8949	0.21911454	0.28424783	0.05481135
2	17.8853	18.8562	18.8351	14.8728	17.5308	18.69715	0.21972978	0.3078664	0.05587409
3	17.8904	18.8903	18.4737	14.8707	17.4904	18.682	0.21999539	0.41312971	0.05702267
4	17.8873	18.9044	18.4241	14.8734	17.5039	18.68425	0.21911538	0.47883954	0.05877438
5	17.8849	18.8102	18.378	14.8718	17.5138	18.8448	0.21870422	0.52578442	0.05722941
6	17.8859	18.8328	18.3287	14.875	17.5238	18.82875	0.21871483	0.8888735	0.05828473

TABLE B2. PROBE CALIBRATION RAW DATA X = 0.26 - 0.37

ANZLE (deg)	P1 (psa)	P2 (psa)	P3 (psa)	PSTAT(psa)	PTOT(psa)	P2 & P3 avg	X	GAMMA	BETA
-5	19.2303	17.6324	17.93781	14.9019	19.5151	17.765105	0.26507724	-0.21132788	0.07515187
-4	19.2236	17.6613	17.88121	14.8884	19.0381	17.781255	0.26522208	-0.13860066	0.07520291
-3	19.2013	17.7207	17.82441	14.8889	18.8791	17.77255	0.26475814	-0.07288818	0.07440878
-2	19.2342	17.7631	17.78881	14.8611	18.98	17.788455	0.26554185	-0.00463479	0.07526931
-1	19.2042	17.83	17.69661	14.8231	18.9864	17.764305	0.26492238	-0.09124971	0.07497813
0	19.2137	17.9099	17.63951	14.8948	18.9402	17.774705	0.26488987	-0.1870197	0.07489492
1	19.221	17.9482	17.57691	14.8648	18.0201	17.783005	0.26527365	-0.26060007	0.07354212
2	19.2201	17.9827	17.50731	14.9019	18.919	17.750005	0.26481125	-0.33017554	0.07484738
3	19.2022	18.0347	17.43671	14.9005	18.0362	17.735705	0.2643806	-0.40776818	0.0763712
4	19.2302	18.0481	17.34001	14.8987	18.0358	17.694055	0.26518222	-0.46995258	0.07988015
5	19.233	18.1032	17.26101	14.9018	19.0197	17.697105	0.26515786	-0.52488568	0.07937378
6	19.2483	18.115	17.2141	14.9034	18.9288	17.688205	0.26544324	-0.58924601	0.08190472
-5	20.7578	18.889	19.0578	14.9191	20.5555	18.8633	0.30008337	-0.20612208	0.09126689
-4	20.7889	18.7415	19.0014	14.8189	20.5097	18.87145	0.3007079	-0.1355446	0.09223432
-3	20.7824	18.8349	18.9218	14.9235	20.5139	18.87825	0.3004684	-0.04553213	0.09148292
-2	20.7886	18.9028	18.8654	14.9229	20.5158	18.884	0.30081477	-0.01963186	0.09161752
-1	20.7828	18.9754	18.7987	14.9318	20.5023	18.88605	0.30023813	-0.09421379	0.09128537
0	20.8028	19.0234	18.7096	14.930	20.5472	18.8865	0.30053062	-0.16208166	0.09307882
1	20.7701	19.0677	18.6358	14.9234	20.5548	18.88675	0.30021511	-0.24267739	0.09163894
2	20.7921	19.134	18.539	14.9278	20.5648	18.838	0.30095141	-0.30468978	0.094079
3	20.7837	19.1791	18.4288	14.941	20.41	18.80385	0.29957054	-0.38292747	0.09438828
4	20.7887	19.2317	18.3189	14.9352	20.5188	18.7753	0.30028045	-0.45338247	0.09695099
5	20.7878	19.291	18.2392	14.9303	20.5395	18.7551	0.29989869	-0.4927709	0.09691445
6	20.7458	19.2888	18.1407	14.9357	20.4787	18.7148	0.29935007	-0.56533727	0.09789933
-5	22.8389	20.289	20.7481	15.009	22.4401	20.52355	0.33781229	-0.18608988	0.10521892
-4	22.8201	20.3708	20.6378	14.9669	22.5798	20.5043	0.33783984	-0.11052739	0.10540084
-3	22.823	20.4329	20.5426	15.0286	22.6422	20.48735	0.33784505	-0.04504871	0.10623608
-2	22.8085	20.5355	20.4681	15.003	22.5493	20.5008	0.33748501	-0.02848151	0.10502250
-1	22.8412	20.6033	20.3866	15.0114	22.6714	20.48495	0.33782282	-0.09636841	0.10708762
0	22.8368	20.6618	20.257	15.008	22.4862	20.4594	0.33786828	-0.16326531	0.10808781
1	22.8358	20.728	20.1875	15.0051	22.8154	20.47055	0.33787852	-0.24580729	0.10746535
2	22.8871	20.8813	20.0801	15.005	22.4924	20.4757	0.33840443	-0.30544843	0.10947691
3	22.9706	20.9014	19.9547	14.9987	22.8625	20.42805	0.33881829	-0.3724273	0.11068714
4	22.9307	20.9408	19.8011	15.0055	22.8417	20.37085	0.33779839	-0.44514327	0.11163418
5	22.9278	20.9803	19.7248	15.0059	22.5477	20.34245	0.3378876	-0.47794388	0.11276436
6	22.8087	21.0078	19.6188	15.0087	22.517	20.3133	0.3373749	-0.5349719	0.11333181
-5	25.185	21.9479	22.461	15.0728	24.9008	0.36935388	-0.17214844	0.11834624	
-4	25.1712	22.0485	22.3855	15.0751	24.8853	22.207	0.36912206	-0.1094285	0.11778157
-3	25.2089	22.1735	22.2919	15.0745	24.8858	22.2327	0.36908072	-0.0393002	0.1179915
-2	25.1828	22.2858	22.2185	15.0789	25.0103	22.24115	0.36923615	-0.10167593	0.11681187
-1	25.2425	22.3807	22.0764	15.0788	24.9345	22.22855	0.37002847	-0.10068385	0.11839982
0	25.2568	22.4609	21.9726	15.0715	24.994	22.21875	0.37005558	-0.18174605	0.11962943
1	25.2548	22.6098	21.8043	15.074	24.9466	22.25751	0.37028925	-0.23537881	0.11810722
2	25.2328	22.6294	21.7488	15.0771	24.87	22.189	0.36989508	-0.28936406	0.1206321
3	25.2277	22.8876	21.5981	15.0747	25.0219	22.14265	0.36987942	-0.35137763	0.12224027
4	25.2882	22.8057	21.4402	15.0883	25.0401	22.12285	0.37052159	-0.42990948	0.12554745
5	25.2022	22.8202	21.3164	15.0737	24.9898	22.0893	0.3696452	-0.47984938	0.12435026
6	25.278	22.8017	21.2615	15.0831	24.7932	22.0818	0.37033101	-0.51246106	0.12838078

## APPENDIX C. APPLICATION OF THE CALIBRATION

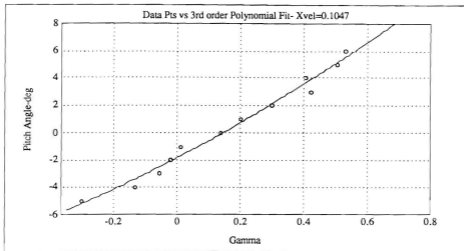


Figure C1. Pitch Angle vs. Gamma X = 0.1047

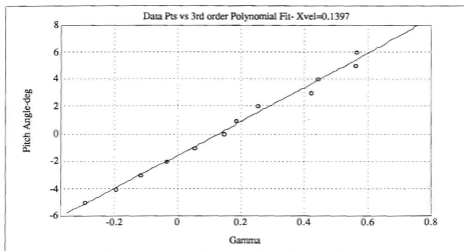


Figure C2. Pitch Angle vs. Gamma X = 0.1397

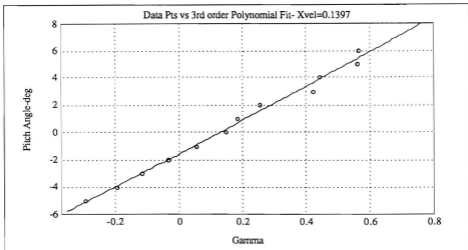


Figure C3. Pitch Angle vs. Gamma X = 0.1812

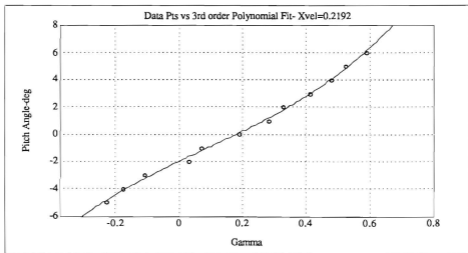


Figure C4. Pitch Angle vs. Gamma X = 0.2192

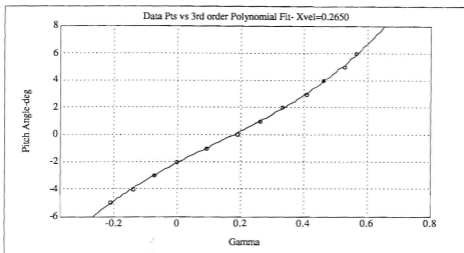


Figure C5. Pitch Angle vs. Gamma X = 0.2650

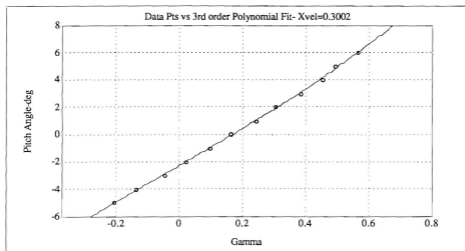


Figure C6. Pitch Angle vs. Gamma X = 0.3002



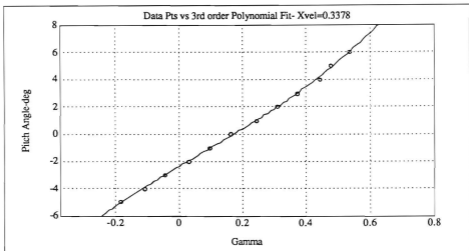


Figure C7. Pitch Angle vs. Gamma  $X = 0.3378$

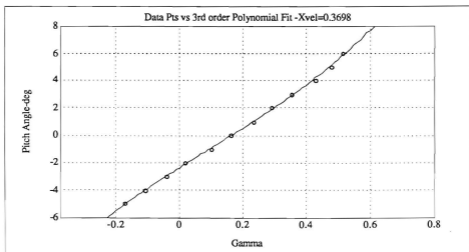


Figure C8. Pitch Angle vs. Gamma  $X = 0.3698$

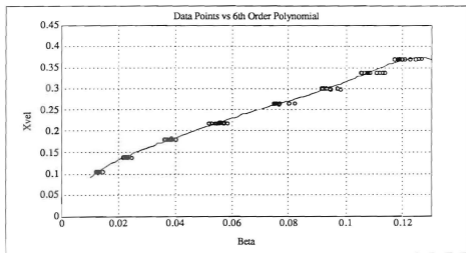


Figure C9. X vs. Beta

TABLE C1. CALIBRATION METHOD RESULTS X = 0.10 - 0.22

ANGLE (deg)	ACTUAL X	CALIBRATED X	CALIBRATED ANGLE	Angle Difference	X % Difference
-5	0.10302443	0.10457949	-5.271	0.271	1.50940746
-4	0.10473655	0.10371192	-3.4375	0.5625	0.97829573
-3	0.10484919	0.10314849	-2.529	0.471	1.62203994
-2	0.10467293	0.10555298	-2.103	0.103	0.84075906
-1	0.10453115	0.10518767	-1.716	0.716	0.62805825
0	0.10450603	0.10124488	-0.109	0.109	3.12053738
1	0.1042947	0.10179391	0.759	0.241	2.39780855
2	0.10553013	0.10596948	2.15	0.15	0.41632236
3	0.10538899	0.10553766	3.93	0.93	0.14107116
4	0.10503711	0.10712581	3.678	0.322	1.98853771
5	0.10499554	0.10698696	5.167	0.167	1.89867253
6	0.10602413	0.11249207	5.517	0.483	6.10044264
-5	0.14025224	0.13980665	-5.09	0.09	0.31770656
-4	0.14079258	0.14122875	-3.91	0.09	0.30979645
-3	0.14012016	0.1382986	-3.01	0.01	1.29999554
-2	0.13922859	0.13791107	-1.988	0.012	0.94630291
-1	0.14051257	0.13841175	-0.919	0.081	1.49511339
0	0.14049581	0.13965073	0.2365	0.2365	0.60149886
1	0.13921777	0.13724023	0.6768	0.3232	1.42046589
2	0.13925365	0.13925365	1.5324	0.4676	2.5999E-06
3	0.1394723	0.1419776	3.647	0.647	1.7962704
4	0.13955706	0.1433869	3.902	0.098	2.74428123
5	0.1388783	0.1443133	5.265	0.265	3.9134965
6	0.13916946	0.14635418	5.55	0.45	5.16257237
-5	0.18166106	0.18007618	-5.124	0.124	0.87243932
-4	0.18176341	0.1800474	-3.92	0.08	0.94408982
-3	0.18238375	0.1818669	-2.749	0.251	0.28338434
-2	0.18097817	0.17639308	-2.231	0.231	2.53350838
-1	0.1811067	0.17862118	-0.8679	0.1321	1.37240608
0	0.18098676	0.1768594	-0.1508	0.1508	2.28047625
1	0.18076512	0.17606679	0.9432	0.0568	2.5996715
2	0.18122165	0.18126723	2.077	0.077	0.02514951
3	0.18102283	0.18117063	2.913	0.087	0.08164354
4	0.18082666	0.18277423	4.608	0.608	1.07703754
5	0.18184116	0.18568528	4.997	0.003	2.22643459
6	0.18128121	0.18634556	5.535	0.465	2.79364135
-5	0.2194901	0.22083929	-4.858	0.142	0.61469162
-4	0.21869114	0.21533631	-4.038	0.038	1.53405034
-3	0.21852929	0.21334476	-3.145	0.145	2.37246331
-2	0.21941948	0.2189379	-1.666	0.334	0.21948013
-1	0.22001366	0.22098927	-1.215	0.215	0.44343307
0	0.219258	0.21775675	0.1151	0.1151	0.68469612
1	0.2191148	0.22028799	1.2	0.2	0.53542175
2	0.21973005	0.22241454	1.789	0.211	1.22127576
3	0.21999585	0.22488684	3.007	0.007	2.22311157
4	0.21911565	0.22438852	4.066	0.066	2.40643095
5	0.21870449	0.22530943	4.899	0.101	3.0200314
6	0.21867328	0.22766856	6.191	0.191	4.11356991

TABLE C2.

CALIBRATION METHOD RESULTS  $X = 0.26 - 0.37$ 

ANGLE (deg)	ACTUAL X	CALIBRATED X	CALIBRATED ANGLE	Angle	
				Difference	% Difference
-5	0.26507717	0.2619759	-5.013	0.013	1.1699502
-4	0.26532291	0.26173636	-3.889	0.111	1.35176715
-3	0.26475806	0.26051754	-2.977	0.023	1.60165967
-2	0.26554158	0.26220618	-2.125	0.125	1.26607285
-1	0.26469231	0.26163475	-0.9976	0.0024	1.15513717
0	0.2648899	0.26147008	0.1185	0.1185	1.29103287
1	0.26507358	0.26274165	0.99788	0.00212	0.87972867
2	0.26481118	0.26459853	1.908	0.092	0.08030137
3	0.26439052	0.26437015	3.039	0.039	0.00770505
4	0.26518215	0.27131254	3.981	0.019	2.31176687
5	0.26515759	0.27126343	5.206	0.206	2.30272106
6	0.26544316	0.27555841	5.9705	0.0295	3.81070088
-5	0.30008337	0.29543526	-4.997	0.003	1.54894039
-4	0.3007079	0.29766971	-4.053	0.053	1.01034686
-3	0.3004684	0.29625409	-2.846	0.154	1.40258162
-2	0.30061477	0.296241	-1.9896	0.0104	1.45494093
-1	0.30023613	0.29543177	-1.004	0.004	1.60019508
0	0.30053062	0.29964959	-0.091	0.091	0.29315864
1	0.30021511	0.29629037	1.001	0.001	1.30730965
2	0.30055141	0.3020306	1.921	0.079	0.49215954
3	0.29957054	0.30277494	3.09	0.09	1.06966512
4	0.30026045	0.30883693	4.23	0.23	2.85634722
5	0.2999689	0.3089709	4.889	0.111	3.0103945
6	0.29935007	0.31149122	6.2	0.2	4.05583392
-5	0.33781195	0.33103523	-5.013	0.013	2.0606283
-4	0.33783959	0.33154321	-3.888	0.112	1.86372124
-3	0.33764471	0.33385295	-2.965	0.035	1.12300352
-2	0.33746468	0.33049924	-1.944	0.056	2.06404389
-1	0.33762227	0.3361555	-1.037	0.037	0.49336794
0	0.33786784	0.33898174	-0.123	0.123	0.32965667
1	0.33787817	0.33725878	1.039	0.039	0.18331802
2	0.33840408	0.34005809	1.998	0.002	0.48876627
3	0.33861794	0.34611675	3.037	0.037	2.21453438
4	0.33779804	0.3486671	4.32	0.32	3.21762102
5	0.33786715	0.35165497	4.95	0.05	4.08084063
6	0.33737456	0.35312697	6.103	0.103	4.66911618
-5	0.36936742	0.36484632	-4.995	0.005	1.22401028
-4	0.36912224	0.36361324	-3.942	0.058	1.49245984
-3	0.3696089	0.36409248	-2.931	0.069	1.49250252
-2	0.36923632	0.36155338	-2.114	0.114	2.08076611
-1	0.37002864	0.36684095	-0.9156	0.0844	0.86147213
0	0.3700547	0.36725096	-0.0529	0.0529	0.75765544
1	0.37028942	0.36552042	1.007	0.007	1.28791266
2	0.36989523	0.36894668	1.839	0.161	0.25643067
3	0.3698796	0.37124174	2.87	0.13	0.36882666
4	0.37052177	0.37356432	5.209	0.209	0.82115315
5	0.36956438	0.3731039	5.148	0.148	0.95775437
6	0.37034436	0.37357425	5.808	0.192	0.87213134

## APPENDIX D. PROGRAM "NEW\_READ\_ZOCI"

```

10      PROGRAM NEW_READ_ZOCI
20      ! Description: Reads specified data compiled from program BIR (BIRD ZOC)
30      ! by Plot ReadLead
40      ! modified by David Byrne
50      ! modified 5 May 1992
51      ! modified 25 Feb 1993 by Jeff Austin for 3 - post processing in a batch
52      ! to determine dimensions, velocity and deviation angle during flight
53      ! otherwise, Program will also determine (range calculated) as a batch
54      ! spec.
55      !-----
60      CLEAR SCREEN
70      ERASE=15 CBI
80      ! Possible definition and dimension
100     DIM Plot_Labels/ REAL (x,Xf,yo,Yf,ds,Dy,101-1150), Label(50), LabelB
110     DIM STD_Disk_Station_File,Plot_Sample_Station_Sample_Station
120     DIM Plot_Labels_Scan as integer
130     DIM Plot_Labels
140     ! Variable initialization
150     Label=11.896      ! Standard day atmospheric pressure
160     Concn=491151     ! Concentration from 10 to 100 ppb
170     Gamma=1.5       ! Ratio of specific heat
180     T=293.15       ! Sub-Ambient Temp
190     alt=0
200     ! Dimension string variable for data location
210     DIM Data_disc(125)
220     DIM Data_disc2(125)
230     !
240     !-----
250     !HOT KEY ROUTINES AND INITIAL SCREEN DISPLAY
260     !-----
270     !
280     ON KEY 1 LABEL *ZOC   INPUT   * GOTO Input
290     ON KEY 3 LABEL *PRINT DATA * GOTO Print
300     ON KEY 4 LABEL *PL   PLOT     * GOTO Pl
310     ON KEY 6 LABEL *H   *        * GOTO Hold
320     ON KEY 7 LABEL *    *        * GOTO Hold
330     ON KEY 8 LABEL *EXIT  FROM   * GOTO Finish
340     !
350     !-----
360     ! INITIAL SCREEN DISPLAY
370     !-----
380     !
390     !
400     !
410     Events = 1
420     CLEAR SCREEN
430     PRINT
440     PRINT
450     PRINT *      READ ZOC DATA AND DISPLAY AS SHOWN
460     PRINT
470     PRINT *      Input ZOC information and read data      F1
480     PRINT *      Print data to CBI or PRINTER             F2
490     PRINT *      Plot Data/Print Losses                   F5
500     PRINT *      Print out ZOC and Deviation Angle
510     PRINT *      as Vertical Distance Traversed (BIRD READ)
520     PRINT
530     PRINT
540     PRINT *      Exit Program                               F9
550     PRINT
560     !
570     Hold = 1
580     GOTO Hold

```

Figure D1. Program "NEW\_READ\_ZOCI"









```

1400 ALLOCATE REAL P(1:100) * Contd.
4064 ALLOCATE REAL P3(nc1:Scan_max)
4065 ALLOCATE REAL P4(nc1:Scan_max)
4066 ALLOCATE REAL P5(nc1:Scan_max)
4068 I PA IS PI in the current probe.
4070 INTEGER N pla,L,K,Dev
4071 K=nc1
4072 ALLOCATE REAL P2(nc1:Scan_max) Used in Language Interact 1989.
4073 ALLOCATE REAL P6(nc1:Scan_max)
4074 ALLOCATE REAL P7(nc1:Scan_max)
4075 ALLOCATE REAL P8(nc1:Scan_max)
4076 ALLOCATE REAL P9(nc1:Scan_max)
4077 ALLOCATE REAL P10(nc1:Scan_max)
4078 ALLOCATE REAL P11(nc1:Scan_max)
4079 ALLOCATE REAL P12(nc1:Scan_max)
4080 ALLOCATE REAL P13(nc1:Scan_max)
4081 ALLOCATE REAL P14(nc1:Scan_max)
4082 ALLOCATE REAL P15(nc1:Scan_max)
4083 ALLOCATE REAL P16(nc1:Scan_max)
4084 ALLOCATE REAL P17(nc1:Scan_max)
4085 ALLOCATE REAL P18(nc1:Scan_max)
4086 ALLOCATE REAL P19(nc1:Scan_max)
4087 ALLOCATE REAL P20(nc1:Scan_max)
4088 ALLOCATE REAL P21(nc1:Scan_max)
4089 ALLOCATE REAL P22(nc1:Scan_max)
4090 I
4091 *****
4092 I
4093 Plot=1
4094 I
4095 Initialize plot parameters
4096 IHE=1
4097 Title="Vertical Distance Inversend vs. P2"
4098 X_Labels="Total Pressure [psi]"
4099 Y_Labels="Vertical Distance [in]"
4100 X=30
4101 Y=60
4102 Y=2
4103 Y=0
4104 O=-25
4105 O=-32
4106 PAI Pen2= (-1)
4107 PAO21=2
4108 Pen21:Scan_max)=2
4109 I
4110 LOWI Plot Sets up graphics environment
4111 I
4112 "Fica quantities calculated and total pressure plotted.
4113 I
4114 G=27.2
4115 G=5.3
4116 I
4117 I Read in data of new blade survey positions.
4118 DATA 0.0625,0.125,0.1875,0.25,0.3125,0.375,0.4375,0.500,0.5625,
,625,0.6875,0.75,0.8125,0.875,0.9375,1.0,1.0625,1.125,1.1875,1.25,1.3125,1.375,1.4375,1.500,1.5625
4119 DATA 0.96875,1.0,1.1,1.125,1.15,1.175,1.2,1.225,1.25,1.275,1.3,1.325,1.35,1.375,1.4,1.425,1.45,1.475,1.5
4120 DATA 0.96875,1.0,1.1,1.15,1.2,1.25,1.3,1.35,1.4,1.45,1.5,1.55,1.6,1.65,1.7,1.75,1.8
4121 I
4122 I
4123 FOR I=1 TO Scan_max
4124 P(nc1+I)=Pa(29,I)
4125 P(nc1+I+1)=Pa(30,I)
4126 P(nc1+I+2)=Pa(31,I)
4127 P(nc1+I+3)=Pa(32,I)
4128 I
4129 I
4130 OI3)=P(nc1+I)-I(nc1+I)

```

Figure D1. (cont) Program "NEW\_READ\_ZOC1"



```

5620 IF X <= X_val(1) THEN X_val = X_val(1) AND X = X_val(1)
5621 X_upper = X_val(4)
5622 Phi_upper = Phi_4(1)
5623 Phi_lower = Phi_3(1)
5624 END IF
5625 IF X <= X_val(1) THEN X_val = X_val(1) AND X = X_val(1)
5626 X_upper = X_val(4)
5627 Phi_upper = Phi_4(1)
5628 Phi_lower = Phi_3(1)
5629 END IF
5630 IF X <= X_val(5) THEN X_val = X_val(5) AND X = X_val(5)
5631 X_upper = X_val(8)
5632 Phi_upper = Phi_5(1)
5633 Phi_lower = Phi_4(1)
5634 END IF
5635 IF X <= X_val(6) THEN X_val = X_val(6) AND X = X_val(6)
5636 X_upper = X_val(9)
5637 Phi_upper = Phi_6(1)
5638 Phi_lower = Phi_5(1)
5639 END IF
5640 IF X <= X_val(7) THEN X_val = X_val(7) AND X = X_val(7)
5641 X_upper = X_val(10)
5642 Phi_upper = Phi_7(1)
5643 Phi_lower = Phi_6(1)
5644 END IF
5645 IF X <= X_val(8) THEN X_val = X_val(8) AND X = X_val(8)
5646 X_upper = X_val(11)
5647 Phi_upper = Phi_8(1)
5648 Phi_lower = Phi_7(1)
5649 END IF
5650 ! Lagrange interpolation to find the deviation angle
5651 Yans = x(1)
5652 Yans = 0
5653 X_interp(1) = X_lower
5654 X_interp(2) = X_upper
5655 F_interp(1) = Phi_lower
5656 F_interp(2) = Phi_upper
5657 FOR I = 1 TO N_pts
5658 J = I
5659 FOR K = 1 TO N_pts
5660 IF I = K THEN
5661 GOTO 5664
5662 END IF
5663 Z = 2*(X_val(K) - X_interp(I)) / (X_interp(J) - X_interp(I))
5664 NEXT K
5665 Yans = Yans + Z*(F_interp(J) - F_interp(I))
5666 NEXT I
5667 Phi = Phi + 1.0 * Yans
5668 PRINT I
5669 *****
5670 Phi = Phi * coefficient calculation in this position
5671 *****
5672 ! Final Static calculated above.
5673 FOR I = 1 TO Scan_num
5674 Plot F_val(I), X(I), Pen(1)
5675 NEXT I
5676 PAUSE
5677 CLEAR SCREEN
5678 !Print results to Print-Jel
5680 PRINT# 15, CR
5681 INPUT "Deviation angle and X_val data to CR1 or Printer: (0=CR1, 1=Printer) =
5682 IF Dev = 1 THEN PRINTER IS 102
5683 CLEAR SCREEN
5684 !

```

Figure D1 (cont) Program "NEW\_READ\_ZOC1"



```

7241 X_val(1)=2*(1/3)*Gamma+1/3*(1+X_val(1))**2*(Gamma-1)**3
5748 I3_dant(1)=X1_ref(1)**2*(1-X1_ref(1))**2*(1/3)*(Gamma-1)
5750 I3_array(1)=I3_num(1)/I3_dant(1)
5751 I
5752 NEXT I
5753 I Begin calling subroutines to determine proper interval of integration
5754 Lcpoint1=1
5755 Rpoint1=33
5756 CALL StackFlus(Lcpoint1,Rpoint1,I3_array(+),Y(+),I1_int_Posit1,Low1,High1,
e1,Value7,High1,Low1)
5757 PRINT "VALUE1="Value1
5758 PRINT "VALUE2="Value2
5759 PRINT "I1="High1
5760 PRINT "I1="Low1
5761 I Return the index values to interpolate between when calculating I1,I2,I3
5762 I interpolate to find proper traverse position for our blade space
5763 Xa_1=1+R
5764 PAUSE
5765 CALL Interpolate(Value1,Value2,Posit1,Posit2,Probe_posit1,Xa_1)
5766 PRINT "Probe position for one blade space ="(Probe_posit1)
5770 PAUSE
5771 I BEGIN VALUES TO CHECK SUBPROGRAMS
5772 I Probe_posit1=.5345
5773 I *****
5774 I Begin calculations of I1,I2,I3 by calling Det_int subprogram
5775 I Define the upper and lower points of the integrals
5776 Lcpoint1=1
5777 CALL Det_int(Lcpoint1,High1,I1_array(+),Y(+),I1_int_lo,hi)
5778 CALL Det_int(Lcpoint1,Low1,I1_array(+),Y(+),I1_int_lo)
5779 CALL Interpolate(Value1,Value2,I1_int_lo,I1_int_hi,I1_int,Xa_1)
5780 PRINT "I1_INT="I1_int
5785 PAUSE
5786 I
5787 CALL Det_int(Lcpoint1,High1,I2_array(+),Y(+),I2_int_hi)
5788 CALL Det_int(Lcpoint1,Low1,I2_array(+),Y(+),I2_int_lo)
5789 CALL Interpolate(Value1,Value2,I2_int_lo,I2_int_hi,I2_int,Xa_1)
5790 PRINT "I2_INT="I2_int
5795 PAUSE
5796 I
5797 CALL Det_int(Lcpoint1,High1,I3_array(+),Y(+),I3_int_hi)
5798 CALL Det_int(Lcpoint1,Low1,I3_array(+),Y(+),I3_int_lo)
5799 CALL Interpolate(Value1,Value2,I3_int_lo,I3_int_hi,I3_int,Xa_1)
5800 PRINT "I3_INT="I3_int
5805 PAUSE
5806 REAL P1_ref_avg
5807 REAL X_ref_avg
5808 REAL Q_ref_avg
5809 REAL F_ref_avg
5810 X_ref_avg=0
5811 P1_ref_avg=0
5812 Q_ref_avg=0
5813 F_ref_avg=0
5814 FOR I=1 TO High1
5815 X_ref_avg=X1_ref(I)*X_ref_avg
5816 P1_ref_avg=P1_ref(I)*P1_ref_avg
5817 Q_ref_avg=Q_ref(I)*Q_ref_avg
5818 F_ref_avg=F_ref(I)*F_ref_avg
5819 NEXT I
5820 X_ref_avg=X_ref_avg/High1
5821 P1_ref_avg=P1_ref_avg/High1
5822 Q_ref_avg=Q_ref_avg/High1
5823 F_ref_avg=F_ref_avg/High1
5824 I
5825 I *****using I1,I2,I3 calculate A,B,C,D,E
5826 A=(I2_int/I1_int)*X_ref_avg
5827 B=(I3_int/I1_int)*X_ref_avg
5828 C=(Gamma+1)/(Gamma-1)**2

```

Figure D1. (cont) Program "NEW\_READ\_ZOCI"

```

6216 D1=2*SQRT(D1)+1-(12*Gamma)/(Gamma+1)*A1/2) B1/2
6217 E1=0.17*A1/24(1-(2*Gamma)/(Gamma+1)*A1/2)1/2
6219 X3_sub=SQRT(1-D1+SQRT(D1)*2+4*C1+E1)/(2*C1)
6220 X3_sub=SQRT(1-D1+SQRT(D1)*2+4*C1+E1)/(2*C1)
6221 PRINT 'X3 SUB =',X3_sub
6222 X3_mixed=X3_sub
6223 DEG
6224 Beta3_mixed=ASN(A1/2/X3_mixed)
6225 P1=0/P1_ref_avg*X_ref_avg+1-X_ref_avg/3/((Gamma+1)*X_ref_avg)
6226 X3_mixed=1+(1-1/(Gamma+1))*COS(Beta3_mixed)
6227 P1=1+(1-1/(Gamma+1))*SQRT(1-X_ref_avg/3/((Gamma+1))*COS(Beta3_mixed))
6228 Q_mixed=P1_ref_avg/P1/3/1/Q_ref_avg)
6229 IFB1 'Device in print routine (0=CRT 1=INTER) 0=
6230 IF G=0 THEN PRINT PRINTER IS 022
6231 CLEAR SCREEN
6232 PRINT '14 UPPER =',beta3_mixed
6233 PRINT '14 LOWER =',beta3_mixed
6234 PRINT 'X3_mixed =',X3_mixed
6235 PRINT 'P1_ref_avg =',P1_ref_avg
6236 PRINT 'P13_mixed =',P13
6237 PRINT 'Beta3_mixed =',beta3_mixed
6238 PRINT 'Q_mixed =',Q_mixed
6239 PAUSE
6240 )
6241 ' Plot statistic that was calculated by Newtonian iteration
6242 )
6243 CLEAR SCREEN
6244 PRINT PR IS CRT
6245 CALL PLOT
6246 FOR I=1 TO Scan_max
6247   PLOT P_xint(I),Y(I),Pen2(I)
6248 NEXT I
6249 FOR I=1 TO Scan_max
6250   PLOT P_xl_p(I),Y(I),Pen2(I)
6251 NEXT I
6252 PAUSE
6253 'Deallocate all real variables
6254 )
6255 DEALLOCATE Pen2(*)
6256 DEALLOCATE P_inf(*)
6257 DEALLOCATE P_xint(*)
6258 DEALLOCATE P_ref(*)
6259 DEALLOCATE M_inf(*)
6260 DEALLOCATE M_xint(*)
6261 DEALLOCATE M1(*)
6262 DEALLOCATE M2(*)
6263 DEALLOCATE M3(*)
6264 DEALLOCATE M4(*)
6265 DEALLOCATE Q(*)
6266 DEALLOCATE P1(*)
6267 DEALLOCATE Y(*)
6268 *****
6269 'Deallocate added variables
6270 DEALLOCATE P2_1(*)
6271 DEALLOCATE P_xl_p(*)
6272 DEALLOCATE P_xl_p1(*)
6273 DEALLOCATE P2_2(*)
6274 DEALLOCATE Pitch(*)
6275 DEALLOCATE Pitch_p1(*)
6276 DEALLOCATE X_vel_p1(*)
6277 DEALLOCATE X_vel(*)
6278 DEALLOCATE Beta_p1(*)
6279 DEALLOCATE Gamma_p1(*)
6280 DEALLOCATE X_interpl(*)

```

Figure D1. (cont) Program "NEW\_READ\_ZOCI"



```

0000 101P100          LABEL = axes label number
0005 1000 0          (Y-axis label)
0010 1000 0.50      (Height label to be printed in plot area)
0015 1000 0          (Ch. ref. p.101.41) code
0020 1000 0          (Sets origin screen size)
0030 01EMPR1 10.90-0010_10_90 (Box around viewport)
0040 0000 0000      (Z-axis limits in DIPS)
0050 0000 0 0 0000/Dx, 0 0000/Dy, X0, Y0 (Box's center X & Y in DIP)
0060 0000 0 0 0000/Dx, 0 0000/Dy, CF, YF (Box's reference window)
0070 0000 0 0 0000/Dx, 0 0000/Dy, X0, Y0, Dx, Dy, CRR (ISO label dimensions in DIP)
0080 0000 0 0 00 00 (Axis label size)
0090 0000 0,0,1,4 (Number X axis)
0100 1000 0
0110 FOR I=0 TO XF STEP X RANGE/Dx
0120   FOR J=0 TO YF STEP Y RANGE/Dy
0130   LABEL USING 'F,J',I
0140 NEXT J
0150 NEXT I
0160 1000 0
0170 FOR I=0 TO YF STEP Y RANGE/Dy
0180   IF ABS(I)/1.0E-5 THEN 100,
0190   MOVE X0, DY+X0, I
0200   LABEL USING 'F,J',I
0210 NEXT I
0220 0000 0
0230 0000 0
0240 SUBPR1
0250 I
0260 CRR = RANGE/Dx, YF, X0, YF, C-1
0270 (Rotation to plot sources around the local origin described)
0280 by the PLOT statement.
0290 Xd=5+XCF-X0
0300 Yd=5+CYF-Y0
0310 PLOT -Xd, Yd, -2
0320 PLOT -Xd, Yd, -1
0330 PLOT -Xd, Yd, 0
0340 PLOT -Xd, Yd, 1
0350 PLOT -Xd, Yd, 2
0360 SUBPR1

```

Figure D1. (cont) Program "NEW\_READ\_ZOCI"



```

7700  SUB R=INT(1+11*INTEGR Expoint1_Hipoint1_P60  DF*3,DF*3+34  INT J  -11  Count
7710  2_Value1_Value7_INTEGER High_3_Low_1)
7715  GO TO 8040 E
7720  DIB G(100)
7730  DIB G(100)
7740  DIB G(100)
7750  DIB Dint(100)
7760  DIB Dint(int(100))
7770  DIB A= 10)
7780  DIB F= 10)
7790  DIB T= 10)
7800  DIB Dint= 10)
7810  DIB Dint(int= 10)
7811  11_100=0
7820  D=Hipoint1
7825  Goto 1
7830  FOR I=1 TO N
7840  D(I)=1/(Pos(I)+Pos(I-1))+1/(D(I+1)-D(I)+1)/(Pos(I)+Pos(I-1)+1)/(D(I-1)+Pos(I-1)+1)/(D(I)+1)
7850  B(I)=D(I)-D(I-1)/(Pos(I)-Pos(I-1))+1/(D(I)+Pos(I-1)+1)/(D(I)+1)
7860  C(I)=(D(I)+B(I)+Pos(I)-1)/(D(I)+Pos(I))
7870  NEXT I
7880  Dint(1)=D(2)*Pos(2)+3  Pos(1)*3/3,040C(1)+Pos(2)+3  Pos(1)+3/3,040C(1)+3  Pos(1)
7890  Dint(1)=D(N)+Pos(N)+3  Pos(1)+3/3,040C(N)+Pos(N)+3  Pos(1)+3  Pos(1)+3  Pos(1)+3  Pos(1)
7900  FOR I=1 TO N
7910  Dint(I)=D(I)+A(I)+3  Pos(I)+3  Pos(I)+3  Pos(I)+3  Pos(I)+3  Pos(I)+3  Pos(I)+3  Pos(I)+3  Pos(I)
7920  NEXT I
7930  FOR I=1 TO N
7940  IF I=1 THEN Dint(I)=1
7950  IF I=1 THEN Dint(I)=1
7960  Pos(I)=Pos(I-1)
7970  Pos(I)=Pos(I-1)
7980  Value2=14_int
7990  Value1=14_int-Dint(I)
8000  High_1=I
8010  Low_1=I-1
8014  GOTO 8040
8020  END IF
8030  NEXT I
8031  Pos(I)=Pos(I)
8032  Pos(I)=Pos(I-1)
8033  Value2=14_int
8034  Value1=14_int-Dint(N)
8035  High_1=I+1
8036  Low_1=I+1
8040  RETURN

```

Figure D1. (cont) Program "NEW\_READ\_ZOCI"

```

0000 0000 int interpolateX_low, X_high, F_lower, F_upper, Ylow, Yhigh, I
0001 001000 BASE I
0002 0000 0000 0000
0003 0000 0000 0000
0004 0000 0000 0000
0005 0000 0000 0000
0006 0000 0000 0000
0007 0000 0000 0000
0008 0000 0000 0000
0009 0000 0000 0000
0010 0000 0000 0000
0011 0000 0000 0000
0012 0000 0000 0000
0013 0000 0000 0000
0014 0000 0000 0000
0015 0000 0000 0000
0016 0000 0000 0000
0017 0000 0000 0000
0018 0000 0000 0000
0019 0000 0000 0000
0020 0000 0000 0000
0021 0000 0000 0000
0022 0000 0000 0000
0023 0000 0000 0000
0024 0000 0000 0000
0025 0000 0000 0000
0026 0000 0000 0000
0027 0000 0000 0000
0028 0000 0000 0000
0029 0000 0000 0000
0030 0000 0000 0000
0031 0000 0000 0000
0032 0000 0000 0000
0033 0000 0000 0000
0034 0000 0000 0000
0035 0000 0000 0000
0036 0000 0000 0000
0037 0000 0000 0000
0038 0000 0000 0000
0039 0000 0000 0000
0040 0000 0000 0000
0041 0000 0000 0000
0042 0000 0000 0000
0043 0000 0000 0000
0044 0000 0000 0000
0045 0000 0000 0000
0046 0000 0000 0000
0047 0000 0000 0000
0048 0000 0000 0000
0049 0000 0000 0000
0050 0000 0000 0000
0051 0000 0000 0000
0052 0000 0000 0000
0053 0000 0000 0000
0054 0000 0000 0000
0055 0000 0000 0000
0056 0000 0000 0000
0057 0000 0000 0000
0058 0000 0000 0000
0059 0000 0000 0000
0060 0000 0000 0000
0061 0000 0000 0000
0062 0000 0000 0000
0063 0000 0000 0000
0064 0000 0000 0000
0065 0000 0000 0000
0066 0000 0000 0000
0067 0000 0000 0000
0068 0000 0000 0000
0069 0000 0000 0000
0070 0000 0000 0000
0071 0000 0000 0000
0072 0000 0000 0000
0073 0000 0000 0000
0074 0000 0000 0000
0075 0000 0000 0000
0076 0000 0000 0000
0077 0000 0000 0000
0078 0000 0000 0000
0079 0000 0000 0000
0080 0000 0000 0000
0081 0000 0000 0000
0082 0000 0000 0000
0083 0000 0000 0000
0084 0000 0000 0000
0085 0000 0000 0000
0086 0000 0000 0000
0087 0000 0000 0000
0088 0000 0000 0000
0089 0000 0000 0000
0090 0000 0000 0000
0091 0000 0000 0000
0092 0000 0000 0000
0093 0000 0000 0000
0094 0000 0000 0000
0095 0000 0000 0000
0096 0000 0000 0000
0097 0000 0000 0000
0098 0000 0000 0000
0099 0000 0000 0000
0100 0000 0000 0000

```

Figure D1. (cont) Program "NEW\_READ\_ZOC1"

## APPENDIX E. MIXED-OUT LOSS CALCULATION

The calculation of the total pressure loss coefficient in the fan-blade cascade model required the calculation of fully-mixed-out-flow conditions. This requirement was difficult due to the probe not traversing parallel to the trailing edge of the blades, and the use of uneven spacings. Figure E1 shows the fully-mixed-out control volume for the analysis, and the location of the traverse in the fan blade cascade model.

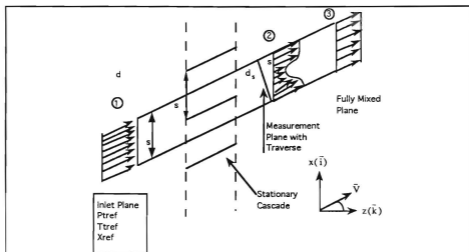


Figure E1. Fully-Mixed-Out Control Volume

The equations for the analysis, reported by Armstrong [Ref. 12], were programmed in HP Basic and are part of the data reduction program "NEW\_READ\_ZOC1" listed in Appendix D. The analysis required that the probe data be taken over a single blade space. Due to the probe traverse not traversing parallel to the trailing edge, it was required that the program calculate when the

probe had measured the same integrated mass flux at position 2 as had entered at position 1 ( where nozzle free-stream conditions were known). The integral in equation 1 was programmed as a subprogram labeled "Mass\_flux".

$$1 = \int_0^{\frac{d_s}{d_1}} \frac{X_2(1-X_2)^{\frac{1}{\gamma-1}}}{X_{ref}(1-X_{ref})^{\frac{1}{\gamma-1}}} \cdot \frac{P_{T2}}{P_{T1}} \cdot \cos \beta_2 d\left(\frac{x}{d_1}\right) \quad (1)$$

where  $d_1$  is the staggered passage width of 1.656 inches and  $d_s$  is the blade traverse distance required for the analysis. By computing the integral at every point in the traverse, the distance  $d_s$  was determined where the integral became unity. Once the proper blade space distance was known the following equations could be calculated using the subprogram "Dat\_int" which was an integration scheme designed to integrate a function over non-equispaced points.

$$\hat{i}_1 = \int_0^1 \frac{X_2(1-X_2)^{\frac{1}{\gamma-1}}}{X_{ref}(1-X_{ref})^{\frac{1}{\gamma-1}}} \cdot \frac{P_{T2}}{P_{Tref}} \cdot \cos \beta_2 d\left(\frac{x}{s}\right) \quad (2)$$

$$\hat{i}_2 = \int_0^1 \frac{X_2^2(1-X_2^2)^{\frac{1}{\gamma-1}}}{X_{ref}^2(1-X_{ref}^2)^{\frac{1}{\gamma-1}}} \cdot \frac{P_{T2}}{P_{Tref}} \cdot \cos \beta_2 \sin \beta_2 d\left(\frac{x}{s}\right) \quad (3)$$

$$\hat{I}_3 = \int_0^1 \frac{\left[ (1-X_2^2)^{\frac{\gamma}{\gamma-1}} + \left( \frac{2\gamma}{\gamma-1} \right) \cdot X_2^2 (1-X_2^2)^{\frac{1}{\gamma-1}} \cdot \cos^2 \beta_2 \right]}{X_{ref}^2 (1-X_{ref}^2)^{\frac{1}{\gamma-1}}} \cdot \frac{P_{T2}}{P_{Tref}} \cdot d\left(\frac{x}{s}\right) \quad (4)$$

$$\hat{A} = X_{ref} \cdot \frac{\hat{I}_2}{\hat{I}_1} = X_3 \sin \beta_3 \quad (5)$$

$$\hat{B} = X_{ref} \cdot \frac{\hat{I}_3}{\hat{I}_1} = \frac{\left[ (1-X_3^2) + \left( \frac{2\gamma}{\gamma-1} \right) X_3^2 \cos^2 \beta_3 \right]}{X_3 \cos \beta_3} \quad (6)$$

$$C = \left( \frac{\gamma+1}{\gamma-1} \right)^2 \quad (7)$$

$$D = 2 \left( \frac{\gamma+1}{\gamma-1} \right) \left[ 1 - \left( \frac{2\gamma}{\gamma-1} \right) \hat{A}^2 \right] - \hat{B}^2 \quad (8)$$

$$E = \left[ 1 - \left( \frac{2\gamma}{\gamma-1} \right) \hat{A}^2 \right]^2 + \hat{A}^2 \hat{B}^2 \quad (9)$$

$$X_3^2 = \frac{-D \pm \sqrt{D^2 - 4CE}}{2C} \quad (10)$$

where the subsonic root of  $X_3$  is chosen

$$\beta_3 = \sin^{-1} \left( \frac{\hat{A}}{X_3} \right) \quad (11)$$

$$P_{T3} = \frac{X_{ref} (1 - X_{ref}^2)^{\frac{1}{\gamma-1}} P_{Tref} \hat{I}_1}{X_3 (1 - X_3)^{\frac{1}{\gamma-1}} \cos \beta_3} \quad (12)$$

The fully-mixed-out loss coefficient could be then be calculated using the inlet total pressure, the fully-mixed-out total pressure, and inlet static pressure in Equation 13.

$$\omega = \frac{P_{tref} - P_{t3}}{P_{tref} - P_{staticref}} \quad (13)$$

When the above procedure was followed using the baseline test data, the values obtained for  $d_s$  were significantly greater than 1.656 inches. In reducing the baseline data, the fully-mixed-out condition was calculated using Eq. (2) - Eq.(12), with the full survey distance (s), which was 1.656 inches.

## APPENDIX F. SELECTED RAW DATA

Data Print Out for Log # 1 , Run # 2 , F1167P141424  
 Period between samples (sec): .0030303030303  
 Sample collection rate (Hz): 330  
 Number of samples per port: 10  
 Length of data run (sec): 31  
 The scan type is: 3  
 Number of scans/traverses: 31  
 Increment of traverse: .0625 inches  
 Atmospheric pressure is: 14.72 psia  
 Tunnel Pressure Ratio is: 2.11030215725

Scan	Port Number						
	1	24	25	29	30	31	32
1	15.410	47.191	45.052	15.463	32.632	53.700	51.635
2	15.410	47.276	45.023	15.483	32.642	53.714	51.607
3	15.390	47.257	44.976	15.473	32.652	53.700	51.550
4	15.443	46.982	44.769	15.483	32.622	53.741	51.704
5	15.399	46.982	44.712	15.533	32.582	53.650	51.170
6	15.399	46.906	44.562	15.543	32.562	53.649	51.112
7	15.377	47.001	44.610	15.483	32.562	53.700	51.100
8	15.356	47.097	44.741	15.503	32.602	53.694	51.200
9	15.421	47.096	44.684	15.513	32.542	53.696	51.312
10	15.291	46.782	44.429	15.513	32.482	53.688	50.921
11	15.356	46.915	44.543	15.513	32.562	53.700	51.055
12	15.388	47.343	44.901	15.473	32.482	53.714	51.493
13	15.387	47.428	44.910	15.463	32.582	53.677	51.607
14	15.453	46.372	43.644	15.533	32.522	53.650	50.433
15	15.399	42.269	40.175	15.503	32.952	53.641	45.396
16	15.410	41.344	39.451	15.493	32.542	53.632	43.554
17	15.432	38.783	38.000	15.463	32.582	53.741	40.895
18	15.345	41.919	41.625	15.483	32.532	53.569	44.488
19	15.399	46.239	45.230	15.523	32.582	53.732	50.625
20	15.421	46.801	45.969	15.523	32.682	53.723	51.303
21	15.367	46.744	45.522	15.523	32.532	53.623	51.246
22	15.432	46.649	45.456	15.453	32.502	53.641	51.255
23	15.464	46.582	45.612	15.533	32.472	53.723	51.227
24	15.356	46.497	45.597	15.543	32.512	53.706	51.189
25	15.410	46.439	45.456	15.563	32.482	53.632	50.980
26	15.464	46.420	45.569	15.513	32.522	53.700	51.084
27	15.377	46.296	45.550	15.543	32.552	53.695	51.007
28	15.443	46.382	45.652	15.533	32.482	53.632	51.036
29	15.399	46.229	45.650	15.483	32.502	53.632	51.046
30	15.399	46.373	45.901	15.593	32.512	53.669	51.151
31	15.432	46.277	46.053	15.543	32.462	53.705	51.170
32	15.443	46.105	46.205	15.543	32.522	53.695	51.131
33	15.421	46.210	46.195	15.513	32.442	53.650	51.350

Figure F1. Run 2 2/24/94 Raw Data

Position	Rein	Stress	X_val	Plot	$\theta$
-0.00000	+1.105800	+1.387342	+3.355411	+34.004350	+1.7126
+1.06750	+1.105751	+1.411933	+3.327612	+34.046277	+1.8099
+1.12500	+1.105312	+1.421853	+3.291189	+34.103901	+1.9159
+1.18250	+1.104862	+1.409152	+3.247118	+34.167586	+2.0302
+1.24000	+1.104412	+1.395407	+3.205396	+34.236845	+2.1527
+1.31250	+1.103972	+1.379961	+3.166107	+34.311049	+2.2836
+1.37500	+1.103540	+1.362105	+3.129177	+34.389757	+2.4229
+1.43750	+1.103393	+1.343094	+3.104001	+34.472477	+2.5704
+1.50000	+1.103574	+1.324209	+3.102998	+34.559681	+2.7261
+1.56250	+1.104399	+1.307253	+3.102957	+34.651730	+2.8907
+1.62500	+1.104318	+1.292500	+3.108561	+34.748994	+3.0639
+1.68750	+1.104315	+1.280601	+3.108557	+34.852001	+3.2565
+1.75000	+1.105376	+1.267002	+3.111474	+34.960000	+3.4689
+1.81250	+1.107505	+1.250941	+3.107673	+34.073000	+3.7022
+1.87500	+1.091957	+1.231652	+3.107027	+34.095000	+3.9577
+1.93750	+1.072361	+1.207344	+3.106494	+34.123127	+4.2351
+1.00000	+1.042376	+1.456134	+1.101400	+35.104059	+1.0000
+1.06250	+1.051044	+1.108796	+2.135559	+35.007779	+0.0000
+1.12500	+1.046589	+1.205259	+3.100205	+35.005539	+1.0000
+1.18750	+1.009762	+1.240054	+3.116300	+35.073821	+1.0000
+1.25000	+1.009773	+1.239109	+3.116337	+35.071605	+1.0000
+1.31250	+1.011677	+1.228984	+3.121304	+35.007219	+1.0000
+1.37500	+1.011110	+1.206500	+3.110072	+35.103505	+1.0000
+1.43750	+1.100453	+1.174006	+3.110125	+35.116547	+1.0000
+1.50000	+1.098059	+1.195100	+3.113950	+35.150503	+1.0000
+1.56250	+1.098627	+1.167338	+3.115906	+35.152826	+1.0000
+1.62500	+1.098679	+1.146823	+3.116090	+35.208159	+1.0000
+1.68750	+1.098239	+1.143553	+3.112360	+35.207987	+1.0000
+1.75000	+1.098060	+1.075841	+3.111923	+35.075263	+1.0000
+1.81250	+1.097236	+1.078715	+3.098008	+35.071200	+1.0000
+1.87500	+1.097407	+1.038974	+3.100210	+35.007320	+1.0000
+1.93750	+1.097314	+1.020165	+3.100005	+35.009759	+1.0000
+2.00000	+1.100405	+1.002721	+3.117999	+35.105117	+1.0000

The cascade loss coefficient based on inlet dynamic pressure as calculated using mass averaged quantities as shown below.

$P_{t1a1} = 51.7056520157$  PSIA  
 $P_{t1a2} = 50.4893345376$  PSIA  
 $P_{t1-P1} = 30.1956451806$  PSIA  
 $T_{1avg} = 514.5$  deg R  
 $M_{bar} = .084206392192$

Figure F1. (cont) Run 2 2/24/94 Raw Data



```

Data Print Out for Zone # 1, Run # 4, File 201416744
Period between samples (sec): 0.0030303030303
Sample collection rate (Hz): 330
Number of samples per port: 10
Length of data run (sec): 31
The scan type is: 3
Number of scans/inverseport: 33
Increment of Inverseport: 0.0625 Inverseport
Atmospheric pressure (at): 14.715 psia
Tunnel Pressure Ratio (at): 2.09427170609

```

Scan	Port Number						
	1	24	25	29	30	31	32
1	15.097	46.494	44.282	15.312	37.069	62.911	50.017
2	15.140	46.542	44.301	15.222	37.159	62.930	50.009
3	15.053	46.420	44.253	15.277	37.129	62.959	50.296
4	15.042	46.240	43.994	15.207	37.010	62.994	50.457
5	15.195	46.227	43.941	15.307	37.199	62.920	50.190
6	15.086	46.112	43.709	15.272	37.079	62.979	50.129
7	15.075	46.190	43.836	15.282	37.109	62.979	50.237
8	15.107	46.246	43.859	15.312	37.129	62.930	50.275
9	15.107	46.160	43.760	15.282	37.089	62.984	50.209
10	15.075	46.045	43.650	15.242	37.070	62.956	50.064
11	15.031	45.921	43.590	15.292	37.059	62.956	49.977
12	15.107	46.017	43.694	15.292	37.040	62.966	50.064
13	15.031	46.190	43.779	15.282	37.030	62.993	50.209
14	15.006	46.179	43.460	15.262	37.019	62.747	50.035
15	15.075	44.345	41.500	15.252	37.070	62.975	47.564
16	15.031	46.205	39.470	15.282	37.070	62.975	47.771
17	15.064	37.059	37.165	15.302	37.990	62.930	39.193
18	15.140	41.205	41.020	15.292	37.040	62.940	44.225
19	15.129	45.442	44.694	15.282	37.990	62.939	49.736
20	15.107	45.092	44.745	15.282	37.950	62.902	50.472
21	15.107	45.921	44.703	15.282	37.990	62.939	50.514
22	15.129	45.044	44.773	15.292	37.040	62.704	50.429
23	15.053	45.691	44.792	15.292	37.960	62.940	50.343
24	15.140	45.053	44.839	15.302	37.990	62.920	50.367
25	15.107	45.566	44.707	15.282	37.990	62.939	50.227
26	15.107	45.490	44.860	15.323	37.950	62.930	50.290
27	15.053	45.403	45.000	15.292	37.910	62.939	50.227
28	15.064	45.375	44.971	15.312	37.860	62.911	50.210
29	15.009	45.376	45.075	15.312	37.820	62.902	50.227
30	15.097	45.355	45.141	15.282	37.990	62.975	50.295
31	15.107	45.346	45.320	15.302	37.860	62.993	50.242
32	15.104	45.375	45.565	15.302	37.860	62.911	50.450
33	15.086	45.231	45.546	15.302	37.850	62.793	50.410

Figure F2. Run 4 2/24/94 Raw Data

Position	Beta	Gamma	Delta	Epsilon	Theta
+0.00000	+1.06919	+4.07205	+335743	+33.439932	+3.548
+0.06250	+1.07439	+4.09964	+337187	+33.356166	+3.612
+0.12500	+1.06877	+4.01569	+335075	+33.454211	+3.445
+0.18750	+1.07847	+4.37265	+336100	+33.174569	+4.077
+0.25000	+1.07011	+4.23172	+336001	+33.195979	+3.977
+0.31250	+1.04200	+4.44342	+326237	+33.070156	+4.100
+0.37500	+1.03900	+4.462525	+327415	+33.1790172	+4.233
+0.43750	+1.03921	+4.457597	+327471	+33.001072	+4.324
+0.50000	+1.04520	+4.457256	+329117	+33.013029	+4.341
+0.56250	+1.04380	+4.455215	+328732	+33.1562794	+4.299
+0.62500	+1.04480	+4.446434	+329029	+33.460191	+4.147
+0.68750	+1.04030	+4.445915	+327794	+33.531022	+4.122
+0.75000	+1.03950	+4.463457	+327553	+33.740793	+4.430
+0.81250	+1.04172	+4.520485	+328161	+33.579769	+4.500
+0.87500	+0.96681	+5.09904	+209411	+33.523559	+6.705
+0.93750	+0.79337	+5.34907	+270226	+33.001343	+6.317
+1.00000	+0.42896	+4.11459	+192636	+34.331537	+3.093
+1.06250	+0.69499	+0.86222	+250035	+35.228939	+1.056
+1.12500	+0.94875	+1.179722	+303954	+35.426323	+0.990
+1.18750	+1.02192	+2.22420	+322777	+34.344850	+1.680
+1.25000	+1.02727	+2.19231	+324219	+34.265020	+1.628
+1.31250	+1.01532	+2.09210	+320999	+34.465523	+1.687
+1.37500	+1.01325	+1.176241	+320444	+34.454296	+1.650
+1.43750	+1.01580	+1.159021	+321127	+34.400503	+1.701
+1.50000	+1.01350	+1.168822	+320512	+34.369096	+1.649
+1.56250	+1.00172	+1.123711	+317386	+34.624414	+1.626
+1.62500	+1.00061	+0.80032	+317094	+34.662676	+1.175
+1.68750	+1.00457	+0.79940	+318137	+34.566758	+1.195
+1.75000	+0.99596	+0.959878	+315074	+34.765883	+1.429
+1.81250	+1.00239	+0.44425	+317563	+34.668833	+1.633
+1.87500	+0.99511	+0.05189	+315652	+34.665673	+2.121
+1.93750	+0.99856	-0.06082	+313950	+35.051164	+2.563
+2.00000	+0.99613	-0.062773	+315918	+34.889373	3.004

The cascade loss coefficient based on inlet dynamic pressure as calculated using mass averaged quantities as shown below.

$P_{1n1} = 52.8913362148$  P51A  
 $P_{1n2} = 49.7055979741$  P51A  
 $P_{11} - P_1 = 37.6061847212$  P81A  
 $T_{1av} = 513$  deg R  
 $W_{bar} = .0847131241109$

Figure F2. (cont) Run 4 2/24/94 Raw Data

Data Print Out for Zoc # 1 , Run # 5 , FileZR1414245  
 Period between samples (sec): 0030303030303  
 Sample collection rate (Hz): 330  
 Number of samples per port: 10  
 Length of data run (sec): 31  
 The scan type is: 4  
 Number of scans/traverses: 33  
 Increment of traverse: .0625 Inches  
 Atmospheric pressure is: 14.71 psia  
 Tunnel Pressure Ratio is: 2.1263124713

Scan	Port Number						
	01	24	25	29	30	31	
1	14.950	48.017	43.032	14.931	31.742	52.292	49.367
2	14.901	45.873	43.537	14.991	31.767	52.271	49.101
3	14.890	45.576	43.185	14.961	31.677	52.249	49.381
4	14.880	45.643	43.299	15.001	31.717	52.319	49.548
5	14.858	45.518	43.109	14.961	31.667	52.319	49.558
6	14.880	45.681	43.223	14.991	31.707	52.319	49.617
7	14.814	45.614	43.214	15.001	31.677	52.301	49.681
8	14.800	45.768	43.280	14.971	31.635	52.237	49.897
9	14.803	45.662	43.214	14.931	31.595	52.191	49.607
10	14.782	45.624	42.937	14.991	31.646	52.209	49.395
11	14.900	45.182	42.354	15.041	31.667	52.273	49.851
12	14.847	43.819	41.889	15.011	31.635	52.264	47.854
13	14.800	41.840	39.284	14.981	31.646	52.301	44.980
14	14.869	39.783	37.904	14.981	31.677	52.301	42.812
15	14.814	37.954	36.831	14.961	31.506	52.282	39.695
16	14.869	37.259	36.537	14.921	31.687	52.292	39.568
17	14.782	38.152	37.826	15.011	31.586	52.292	39.998
18	14.825	40.715	40.501	14.951	31.536	52.118	43.491
19	14.835	43.348	42.718	14.931	31.576	52.246	47.425
20	14.800	44.826	44.059	14.971	31.667	52.256	49.396
21	14.858	45.326	44.211	14.971	31.626	52.265	49.887
22	14.890	45.326	44.316	14.961	31.616	52.191	49.964
23	14.912	45.288	44.211	15.021	31.566	52.118	49.964
24	14.800	45.345	44.240	14.971	31.616	52.319	50.040
25	14.869	45.269	44.302	15.001	31.595	52.319	49.897
26	14.901	45.249	44.259	14.991	31.636	52.264	49.848
27	14.912	45.269	44.230	14.981	31.566	52.283	49.916
28	14.869	45.230	44.240	14.991	31.595	52.264	49.910
29	14.836	44.999	44.192	14.981	31.586	52.246	49.627
30	14.901	44.961	44.325	15.001	31.546	52.319	49.694
31	14.956	44.990	44.675	15.051	31.667	52.401	49.858
32	14.901	44.913	44.997	15.061	31.536	52.200	49.973
33	14.912	44.711	45.053	15.011	31.566	52.209	49.983

Figure F3. Run 5 2/24/94 Raw Data

Position	Beta	Gamma	X val	Y val	$6.4^\circ - \theta$
+0.00000	+1.100061	+1.481499	+1.338000	+1.100000	01.0000
+1.17500	+1.107031	+1.475216	+1.370744	+1.100000	01.0000
+1.25000	+1.107102	+1.474182	+1.355294	+1.100000	01.0000
+1.37500	+1.104235	+1.470435	+1.320233	+1.100000	01.0000
+1.50000	+1.105448	+1.469386	+1.337700	+1.100000	01.0000
+1.67500	+1.104000	+1.475026	+1.370000	+1.100000	01.0000
+1.85625	+1.106001	+1.465454	+1.333421	+1.100000	01.0000
+1.88750	+1.107499	+1.467900	+1.337541	+1.100000	01.0000
+1.71875	+1.104209	+1.473676	+1.328263	+1.100000	01.0000
+1.75000	+1.103370	+1.472747	+1.326866	+1.100000	01.0000
+1.78125	+1.103999	+1.465679	+1.327600	+1.100000	01.0000
+1.81250	+1.099897	+1.468371	+1.316630	+1.100000	01.0000
+1.84375	+1.096630	+1.468125	+1.308205	+1.100000	01.0000
+1.87500	+1.096380	+1.466486	+1.264387	+1.100000	01.0000
+1.90625	+1.097994	+1.467907	+1.277030	+1.100000	01.0000
+1.93750	+1.094391	+1.462427	+1.193474	+1.100000	01.0000
+1.96875	+1.095823	+1.462186	+1.200724	+1.100000	01.0000
+1.00000	+1.096294	+1.074027	+1.244407	+1.096294	01.0000
+1.03125	+1.092627	+1.144428	+1.200607	+1.092627	01.0000
+1.06250	+1.099986	+1.153376	+1.316897	+1.099986	01.0000
+1.09375	+1.102500	+1.107040	+1.323946	+1.102500	01.0000
+1.12500	+1.102920	+1.196521	+1.324765	+1.102920	01.0000
+1.15625	+1.104184	+1.206836	+1.320193	+1.104184	01.0000
+1.18750	+1.104871	+1.210690	+1.330003	+1.104871	01.0000
+1.21875	+1.103263	+1.207073	+1.325674	+1.103263	01.0000
+1.25000	+1.102192	+1.194471	+1.322773	+1.102192	01.0000
+1.28125	+1.103496	+1.200091	+1.326310	+1.103496	01.0000
+1.31250	+1.101802	+1.195161	+1.321938	+1.101802	01.0000
+1.34500	+1.101374	+1.168414	+1.320576	+1.101374	01.0000
+1.38750	+1.101646	+1.125889	+1.321303	+1.101646	01.0000
+1.42500	+1.100792	+1.062604	+1.319075	+1.100792	01.0000
+1.46250	+1.100422	+1.016691	+1.318046	+1.100422	01.0000
+2.00000	+1.102052	+1.067175	+1.322395	+1.102052	01.0000

Figure F3. (cont) Run 5 2/24/94 Raw Data

## LIST OF REFERENCES

1. McCormick, D., "Shock-Boundary Layer Interaction Control with Low-Profile Vortex Generators and Passive Cavity", AIAA Paper 92-0064, January 1992.
2. United Technologies Research Center Report R90-957946-13, Transonic Fan Shock Boundary Layer Separation Control, April 1990.
3. Collins, C., Preliminary Investigation of the Shock-Boundary Interaction in a Simulated Fan Passage, M.S.A.E. Thesis, Naval Postgraduate School, Monterey, California, March 1991.
4. Golden, W., Static Pressure Measurements of the Shock-Boundary Layer Interaction in a Simulated Fan Passage, M.S.A.E. Thesis, Naval Postgraduate School, Monterey, California, March 1992.
5. Myre, D., Model Fan Passage Flow Simulation, M.S.A.E. Thesis, Naval Postgraduate School, Monterey, California, December 1992.
6. Tapp, E., Development of a Cascade Simulation of a Fan-Passage Flow, M.S.A.E. Thesis, Naval Postgraduate School, Monterey, California, December 1993.
7. AGARD-AG-207, Modern Methods of Testing Rotating Components of Turbomachines (Instrumentation), by Sieverding, C., 1975.
8. Geopfarth, R., Development of a Device for the Incorporation of Multiple Scanivalves into a Computer-Controlled Data System, M.S.A.E. Thesis, Naval Postgraduate School, Monterey, California, March 1979.
9. Neuhoff, F., Calibration and Application of a Combination Temperature-Pneumatic Probe for Velocity and Rotor Loss Distribution Measurements in a Compressor, BDM Corporation, Contractor Report, December 1981.
10. Nakamura, S., Applied Numerical Methods with Software, Prentice-Hall, Inc., Englewood Cliffs, New Jersey, 1991.
11. Holman, J., Experimental Methods for Engineers, Fifth Edition, McGraw-Hill, Inc., 1989.
12. Armstrong, J., Near-Stall Loss Measurements in a CD Compressor Cascade with Exploratory Leading Edge Flow Control, M.S.A.E. Thesis, Naval Postgraduate School, Monterey, California, June 1990.

13. Shreeve, R., Elazar, Y., Dreon, J., and Baydar, A., "Wake Measurements and Loss Evaluation in a Controlled Diffusion Compressor Cascade", Transactions of the ASME, Journal of Turbomachinery, Vol. 113, No. 4, pp. 591-599, October 1991.

## INITIAL DISTRIBUTION LIST

- |   |         |
|---|---------|
| 1. Defense Technical Information Center<br>Cameron Station<br>Alexandria, Virginia 22304-6145   | 2       |
| 2. Library, Code 52<br>Naval Postgraduate School<br>Monterey, California 93943-5002   | 2       |
| 3. Department of Aeronautics and Astronautics<br>Naval Postgraduate School<br>Monterey, California 93943-5002<br>ATTN: Chairman<br>ATTN: Code AA/SF | 1<br>10 |
| 4. Commanding Officer<br>Naval Aircraft Warfare Center<br>Aircraft Division<br>Trenton, New Jersey 08628-0176<br>ATTN: S. Clouser                   | 1       |
| 5. Naval Air Systems Command<br>Washington, D.C. 20361<br>ATTN: AIR-536T  | 1       |
| 6. Office of Naval Research<br>800 North Quincy Street<br>Arlington, Virginia 22217<br>ATTN: Spiro Lykoudis   | 1       |
| 7. United Technologies Research Center<br>East Hartford, Connecticut 06108<br>ATTN: Duane McCormick   | 1       |
| 8. Lt. Jeff Austin<br>Operations Department<br>USS Carl Vinson (CVN-70)<br>FPO AP 96629-2840  | 2       |

DUDLEY KNOX LIBRARY  
NAVAL POSTGRADUATE SCHOOL  
MONTEREY CA 93943-5101



GAYLORD S



DUDLEY KNOX LIBRARY



3 2768 00018801 5